Development of a Local Active Noise Control System

Akseli Konttas

School of Electrical Engineering

Thesis submitted for examination for the degree of Master of Science in Technology.

Otaniemi 25.09.2023

Supervisor

Prof. Vesa Välimäki

Advisor

D.Sc. Miikka Tikander

Aalto University
School of Electrical
Engineering

Aalto University
School of Electrical Engineering

Aalto University, P.O. BOX 11000, 00076 AALTO
www.aalto.fi
Abstract of the master's thesis

Author Akseli Konttas

Title Development of a Local Active Noise Control System

Degree programme Master's Programme in Computer, Communication and Information Sciences

Major Acoustics and Audio Technology **Code of major** ELEC3030

Supervisor Prof. Vesa Välimäki

Advisor D.Sc. Miikka Tikander

Date 25.09.2023 **Number of pages** 66 **Language** English

Abstract

Active noise control (ANC) is a technology reducing noise by incorporating secondary sources, producing so called anti-noise. This anti-noise has the same amplitude but inverted phase at all frequencies compared to the primary noise under subject of attenuation, resulting in the two sound fields canceling each other out by the principle of superposition.

The aim of this thesis is to evaluate the feasibility of using a mobile simple single-channel ANC system to reduce broadband noise in a 3D-space. To achieve this, different known ANC algorithms are simulated, and based on the simulations, a physical prototype device is developed and tested. Based on literature review, the only viable solution to the problem is to develop a local feedback ANC system. Local ANC systems minimize sound pressure at a single point in space instead of the entire room, and feedback ANC systems conduct the attenuation without prior knowledge of the incoming noise. Thus, feedback ANC is a prediction problem at its core.

Three algorithms are simulated: leaky filtered-x least mean squares algorithm (LFxLMS), functional link artificial neural network based LFxLMS (FLANN), and wavelet packet transform based LFxLMS (Wavelet). Out of these three, LFxLMS and Wavelet were then tested with the prototype system. Both algorithms achieved over 6 dB reduction on low-frequency fan noise, around 1–3 dB reduction on orchestral music, around 1 dB reduction on traffic noise, but virtually no reduction on speech, depending on measurement location.

The results show that such a feedback local ANC system is able to attenuate noise with strong tonal components but cannot attenuate sound that varies quickly in time. Additionally, it was confirmed that secondary path latency forms the biggest limitation of a feedback ANC system and must be minimized for the system to work well.

Keywords active noise control, acoustic signal processing, digital signal processing, feedback control, adaptive signal processing

Aalto University
School of Electrical
Engineering

Aalto-yliopisto, PL 11000, 00076 AALTO
www.aalto.fi
Diplomityön tiivistelmä

Tekijä Akseli Konttas

Työn nimi Paikallisen aktiivisen melunhallintajärjestelmän kehittäminen

Koulutusohjelma Master's Programme in Computer, Communication and Information Sciences

Pääaine Acoustics and Audio Technology **Pääaineen koodi** ELEC3030

Työn valvoja Prof. Vesa Välimäki

Työn ohjaaja TkT Miikka Tikander

Päivämäärä 25.09.2023 **Sivumäärä** 66 **Kieli** Englanti

Tiivistelmä

Aktiivinen melunhallinta (active noise control, ANC) on tekniikka, jolla voidaan vähentää melua tuottamalla toisiokaiuttimella niin kutsuttua vastamelua. Tällä vastamelulla on sama amplitudi mutta käänteinen vaihe vaimennettavaan primäärimeluun nähden, jolloin nämä kaksi äänikenttää kumoavat toisensa superpositioperiaatteen mukaisesti.

Tämän diplomityön tavoitteena on arvioida yksinkertaisen yksikanavaisen aktiiviseen melunhallintaan perustuvan laitteen käyttökelpoisuutta laajakaistaisen melun vaimentamiseksi 3D-tilassa. Tavoitteen saavuttamiseksi työssä simuloidaan tunnettuja aktiivisen melunhallinnan algoritmeja, ja simulointien pohjalta kehitetään prototyyppilaite. Kirjallisuuskatsauksen perusteella ainoa käytettävissä oleva ratkaisu ongelmaan on kehittää paikallinen takaisinkytketty ANC-järjestelmä. Paikalliset ANC-järjestelmät minimoivat äänenpainetta yhdessä pisteessä koko huoneen sijaan, ja takaisinkytketyt ANC-järjestelmät tuottavat vastamelua ilman ennakkotietoa tulevasta primäärimelusta. Takaisinkytketty ANC on siten pohjimmiltaan ennustamisongelma.

Työssä simuloidaan kolmea algoritmia: vuotava referenssisuodatettu pienimmän neliösumman algoritmi (leaky filtered-x least mean squares, LFxLMS), funktionaaliseen linkkineuroverkkoon perustuva LFxLMS (functional link neural network, FLANN) ja lyhyen aaltomuodon muunnokseen perustuva LFxLMS (wavelet packet transform, Wavelet). Näistä kolmesta LFxLMS ja Wavelet testattiin myös prototyyppijärjestelmällä. Molemmat algoritmit saavuttivat yli 6 dB vaimennuksen matalataajuuksiseen tuuletinmeluun, noin 1–3 dB vaimennuksen orkesterimusiikkiin, ja noin 1 dB vaimennuksen liikennemeluun, mittauspaikasta riippuen. Puheeseen kumpikaan algoritmi ei juuri saavuttanut vaimennusta.

Tulokset osoittavat, että tämänkaltainen takaisinkytketty, paikallinen ANC-järjestelmä pystyy vaimentamaan melua, jolla on vahvat, tasaiset tonaaliset komponentit, mutta ei kykene vaimentamaan nopeasti ajassa muuttuvaa ääntä. Lisäksi tulokset vahvistavat, että toisiotien viive on suurin yksittäinen rajoittava tekijä takaisinkytketyissä ANC-järjestelmissä.

Avainsanat aktiivinen melunhallinta, akustinen signaalinkäsittely, digitaalinen signaalinkäsittely, takaisinkytketty säätö, adaptiivinen signaalinkäsittely

Esipuhe

Oma opiskelijaelämä alkaa tämän opinnäytteen valmistumisen myötä olla vähintäänkin toistaiseksi vihdoin päätöksessään. Diplomityö on ollut ehdottomasti yksi kaikista projekteista, ja ehdottomasti on myös paikallaan kiittää kaikkia, jotka ovat mahdollistaneet sen valmistumista! Laajemmassa mielessä kiitokset tänne asti pääsemisestä kuuluvat silti kyllä todella laajalle joukolle ihmisiä – diplomityöprojekti oli loppupeleissä vain se viimeinen puristus kaiken muun opiskeluaikana koetun jälkeen.

Ensinnäkin, suuri kiitos Vesalle ja Miikalle hyvästä ohjauksesta diplomityöprojektin aikana. Oli ilo tehdä töitä kanssanne ja oppia kokeneemmiltaan! Suurkiitokset myös Janille todella mielenkiintoisesta dippa-aiheesta ja mahdollisuudesta sen toteuttamiseen, sekä kaikista ideoista ja eteenpäin puskemisesta projektin aikana. Se pullollinen hiljaisuutta jäi vielä saavuttamatta, mutta ehkä päästiin askeleen lähemmäs. Kiitos myös kaikille Aallon akustiikan labran työntekijöille.

Kiitos kaikille otaniemeläisille opiskelukavereille, ilman teitä nämä noin seitsemän (!) vuotta olisivat olleet mahdottoman paljon tylsempiä; sekä kiitos kaikille muille kavereille siitä, että elämää on kaikesta Otaniemessä vietetystä ajasta huolimatta löytynyt myös opiskelukuplan ulkopuolelta! Ja erityiskiitokset tikoille ja erityisesti Artulle, Jesselle ja Joonalle kaikista peli- ja leffailloista, viikonloppuretkistä sekä kiivaista väittelyistä; Antille kaikesta aina pakastimen jäätelökiintiöstä huolehtimisesta speksiin mukaan vetämiseen sekä ylipäätään olemisesta; sekä Helenalle kaikesta avusta ja tuesta opiskelujen, eikä vähiten dippatyön aikana.

Kiitos Automaatio- ja systeemitekniikan killalle opiskelija- ja teekkarielämään tutustuttamisesta, sekä erityisesti sen hallituksille 2019 ja ’20 sekä AYY:n yhteisöjaosto Aavalle ’22 vähäunisista öistä ja hyvistä kavereista! Opiskelu todella on ihmisen parasta aikaa.

Viimeisenä – muttei todellakaan vähäisimpänä – on tänne asti pääsemisestä todellakin tarpeen kiittää myös koko perhettä. Kiitos molemmille vanhemmille jopa epäreilun hyvistä eväistä elämään, ja äidille myös kaikesta tuesta ja oikoluvusta diplomityön kanssa. Ja kiitos siskoille seurasta, tuesta, ärsyttämisestä, ylipäätään kaikesta näiden viimeisten 26 vuoden ajalta – mitään en vaihtaisi.

Aika monta kertaa ehdin näiden viimeisen muutaman vuoden aikana todeta "näiden olevan nyt ne viimeiset dipolibileet" joihin osallistun, mutta tänä syksynä se saattoi olla tottakin. Kausi pääsi kuitenkin loppumaan huipulle, kun oltiin tämän kuun alussa aavalaisten kanssa katsomassa Robin Packalenin keikkaa Dipolin parvelta; paha siitä olisikaan enää laittaa paremmaksi. Robinin *Puuttuvaa palasta* mukaillen, *"Dippa takana ja elämä edessä"*!

Otaniemessä 25.9.2023

Akseli Konttas

Contents

Symbols and abbreviations

Signal conventions

$d(n)$	primary noise signal
$\hat{d}(n)$	synthesized primary noise signal
$D(z)$	z-transform of primary noise signal
$e(n)$	error signal
$e_2(n)$	control microphone signal
$E(z)$	z-transform of error signal
$u(n)$	adaptive filter output
$U(z)$	z-transform of adaptive filter output
$x(n)$	reference signal
$\hat{x}(n)$	secondary path filtered reference signal
$X(z)$	z-transform of reference signal
$y(n)$	anti-noise signal
$\hat{y}(n)$	estimated anti-noise signal
$Y(z)$	z-transform of anti-noise signal
$\hat{Y}(z)$	z-transform of estimated anti-noise signal

Symbols

A	high-pass filter
c	speed of sound
D	low-pass filter
$\mathbb{E}[.]$	expected value operator
f	frequency
f_s	sampling frequency, sample rate
H	system response
J	cost function
K	controller order
L	filter length
L_{eq}	equivalent sound pressure level
LP	low-pass filter
n	discrete time index
p	acoustic pressure
P	primary path filter
S	secondary path filter
S_{err}	temporal error on secondary path estimation
$\hat{S}$	estimated secondary path filter
^{T}	transpose operator
t	time
w	adaptive filter weights
W	adaptive filter
z	z-transform variable

α	normalized step size
β	small constant
γ	leaky factor
Δ_S	secondary path latency
λ	wavelength; eigenvalue
μ	learning rate, step size
ξ	mean square error
$\hat{\xi}$	estimated mean square error
σ_x	power of signal x
ϕ	angle; decomposed signal

Abbreviations

2D	two-dimensional
3D	three-dimensional
ANC	active noise control
FIR	finite impulse response
FLANN	functional link artificial neural network
FxLMS	filtered-x least mean squares
IIR	infinite impulse response
IMC	internal model control
LFxLMS	leaky filtered-x least mean squares
LMS	least mean squares
NFxLMS	normalized filtered-x least mean squares
NLMS	normalized least mean squares
SNR	signal-to-noise ratio
SPL	sound pressure level

1 Introduction

Whereas producing sound to any point in a room is an extremely simple procedure using loudspeakers and digital signal processors, producing silence is a much more difficult task – one cannot simply open a bottle full of silence. Such a device would be convenient, though, as excessive noise, that is, unwanted or disturbing sound, negatively affects listeners. Even relatively small noise levels can lead to annoyance and disturbance of sleep, decreased productivity, and decreased overall living comfort [1]–[4]. Moreover, in its most severe form, excessive noise exposure can affect overall health of the population in the form of leading to hearing impairments, decreasing cognitive performances, or even leading to cardiovascular diseases [1]–[4]. Thus, there exists a clear need to control noise.

Traditional *passive noise control* methods work by placing absorptive or reflective matter between the noise source and listener, physically shielding the listener from noise [5]. This is the case in constructing acoustic noise barriers beside highways, placing absorbing matter inside walls, or wearing earplugs. Indeed, this kind of noise control is effective at high frequencies; however, it has poor performance at low frequencies where wavelengths are long, as the absorbing materials should be impractically thick to attenuate those long wavelengths [5].

This weakness can be mitigated by using an *active noise control* (ANC) system, often in conjunction with passive noise control methods. ANC systems incorporate a secondary source, typically a loudspeaker, to create suitable anti-noise to counter the unwanted primary noise. Ideally, this anti-noise and the unwanted primary noise cancel each other out by the principle of superposition, which happens when the two sound fields have the exact same amplitude but phase difference of 180 degrees. ANC methods complement passive noise control methods well as they are most effective at low frequencies at which passive noise control is ineffective [6]. Conversely, performance of ANC systems tend to deteriorate on high frequencies at which passive noise control is effective in turn.

Active noise control has already been researched and used in different applications for decades. Some typical applications of ANC systems are to reduce road and engine noise in high-end cars [7], to reduce propeller noise in passenger cabins in airplanes [6], and to control fan noise in air ventilation ducts [8], [9]. Some more recent applications include active windows [10] and active noise barriers [11]. Furthermore, a major application is active noise control headphones, also called active noise canceling headphones. Compared to passive hearing protection, such as typical earplugs, ANC headphones perform better at lower frequencies. Furthermore, compared to listening to music with normal headphones, ANC headphones are superior in suppressing background noise, giving a more pleasant listening experience. As such, ANC headphones are the subject of extensive research and rapid development [12]–[14].

Even though proven to work, ANC systems tend to be fixed in the single environment for which they were designed and installed to, be it a car, an airplane, or a ventilation duct. In contrast, ANC headphones can be used in any environment, but using headphones is not always practical. Assuming easy usage and adequate performance, there are little downsides in controlling noise without the user having

to wear anything in their ears. Additionally, it has been proved that active noise control in 3D-spaces, such as in office rooms, is indeed possible in theory [15], [16], albeit with limitations.

However, when the system is not fixed to a single space, the existing solutions incorporate large microphone and loudspeaker arrays, rendering them impractical for consumer use. Even if a system with 12 carefully placed loudspeakers would offer similar performance as ANC headphones, few would choose the said system over headphones. Preliminary research did not find attempts to create viable alternatives to ANC headphones, and as such, no attempts have been made to move the headphones from the ears to the table.

Therefore, the aim of this thesis is to evaluate the feasibility of using a mobile, easy-to-use ANC system to reduce broadband noise at a single point in a 3D-space. The core idea behind the system is to produce the aforementioned "silence in a bottle", and using the device would ideally be as simple as placing it on a table and switching it on, leading to perceived silence by the user. To achieve this goal, the thesis will simulate several different known active noise control algorithms. A physical prototype system will be developed based on the simulation results, after which the performance of the system is evaluated. Although ANC systems can in principle have as many sensors and secondary sources as the computational capacity allows, this thesis is limited to use only single-channel ANC, that is, only one secondary source, reference sensor, and error sensor.

The rest of this thesis is organized as follows. Chapter 2 reviews the relevant acoustical background of ANC and introduces different basic ANC system architectures. Chapter 3 introduces the concept of adaptive filtering and presents some known adaptive algorithms and techniques used in active noise control. Chapter 4 derives and justifies the structure and design choices of the resulting ANC system. Chapters 5 and 6 introduce the simulation and prototype systems as well as present results acquired from said systems, respectively, and discuss the results and the feasibility of using such a system. Finally, Chapter 7 concludes this thesis.

2 Principles of active noise control

The core technologies of active noise control have already been researched for decades. The first mention of such an idea appeared already in 1930s, when Paul Lueg patented his idea of silencing sound by destructive interference [17]; unfortunately, this relatively simple idea was difficult to implement with the electronics available back then [18]. Olson and May introduced their idea of electronic sound absorber in 1953 [19], which was essentially an analog local feedback ANC system creating a zone of quiet around an error microphone. However, the modern active noise control research can be seen originating from 1970s, when the first adaptive ANC algorithm [20], filtered-x least mean squares algorithm [21] and first digital signal processors [18] were invented. Even though the research of ANC has taken significant steps in the last fifty years [18], the principle of cancelling out a primary noise signal using a secondary source has remained the same from Lueg's original idea.

This chapter will discuss the basic terminology and fundamentals of active noise control. First, terms and conventions used in this thesis are explained, after which the fundamental acoustics regarding active noise control is presented. Rest of this chapter introduces and explains different ANC system architectures. To these architectures include the division between feed-forward and feedback ANC control systems, and the different effective areas of ANC, called global, local, and spatial ANC.

2.1 Terms and conventions

Terms

In this thesis, the term *noise* is used to refer to any unwanted sound that is subjected to attenuation using an ANC system. As such, noise can mean any kind of audible sound, such as a sinusoidal tone, white or pink noise, environmental noise, speech, or music.

Noise can broadly be divided into two categories, narrowband and broadband noise. Narrowband noise has relatively sharp peaks in its spectrum, while the spectrum of broadband noise is wider [22]. A pure sinusoidal tone is an extreme example of narrowband noise, while white noise is an extreme example of broadband noise.

The unwanted noise is also called *primary noise*, which is radiated from a *primary source*. In practice, there can exist multiple primary sources, in which case primary noise commonly notes the superposition, or sum, of the combined noise radiated from all these primary sources at a single point in space.

Active noise control works by producing suitable *anti-noise*, also called *secondary noise*, to cancel out the primary noise. This anti-noise is emitted by a *secondary source* or *anti-noise source*, which is typically a loudspeaker. ANC systems are commonly adaptive, in which case there are one or more *error sensors*, typically microphones, evaluating the performance of the control. To be precise, the secondary source does not have to be a loudspeaker nor the error sensor a microphone, and other kinds of actuators can also be used instead. However, for consistency and

clarity, the secondary source is in this thesis assumed to be a loudspeaker, and error sensor is assumed to be a microphone.

Signal conventions

Following common practice, signals and impulse responses in time domain are denoted by lower-case letters, while the same signals and impulse responses in Z-domain are written with capital letters. Thus, $x(n)$ denotes a time-domain signal, $\mathbf{w}(n)$ denotes an impulse response, and $X(z)$ denotes the Z-transform of signal x. The index n is the discrete time index.

A short-hand notation of the signals without explicitly writing the dependency of n or z can also be used when unambiguous. Thus, $x \equiv x(n)$ and $S \equiv S(z)$.

Scalars and vectors

In this thesis, scalars are written with non-bolded and vectors with bolded letters. Therefore, $d(n)$ is a scalar value of signal d at time n, while $\mathbf{d}(n)$ is a vector of scalar values. Superscript ^{T} denotes transpose operation: $\mathbf{x}^T$ is transposition of vector $\mathbf{x}$.

2.2 Fundamental acoustics

Sound is pressure waves travelling in a medium. If there are two sound fields p_1 and p_2 having varying pressure fluctuations in spatial coordinates x, y and z in function of time t, the resulting total sound pressure in this position is simply the sum, or *superposition* of these two fields [23]:

$$p_{tot}(x, y, z, t) = p_1(x, y, z, t) + p_2(x, y, z, t). \tag{1}$$

This superposition principle assumes linearity of sound, which is not strictly true. However, the effects of non-linearities are negligent and can safely be discarded, if the amplitudes of the acoustic disturbances are small enough [23]. These non-linear distortions typically become significant first when the sound pressure level is over 120 dB [23]. As the usual range of sound pressure levels present in average person's daily life is around 0 dB – 110 dB [24], the assumption of linearity is usually justified.

The superposition principle shown in equation 1 can be generalized to any number of sound fields and is the main idea behind active noise control. Given a primary noise signal d, the aim of active noise control is to produce an anti-noise signal y such that it has exactly the same amplitude as d but an inverted phase, that is, a phase shift of π radians or 180°. This would lead to a perfect *destructive interference*, canceling out both signals. In contrast, phase of the secondary signal aligning with that of primary signal leads to *additive interference*, in which case the primary signal is amplified by the secondary signal. Figure 1 shows examples of both additive and destructive interferences.

The goal of active noise control is to produce a secondary signal which has the same amplitude but opposing phase on every frequency compared to primary signal, at the measurement location, canceling out both signals. This can be quite difficult

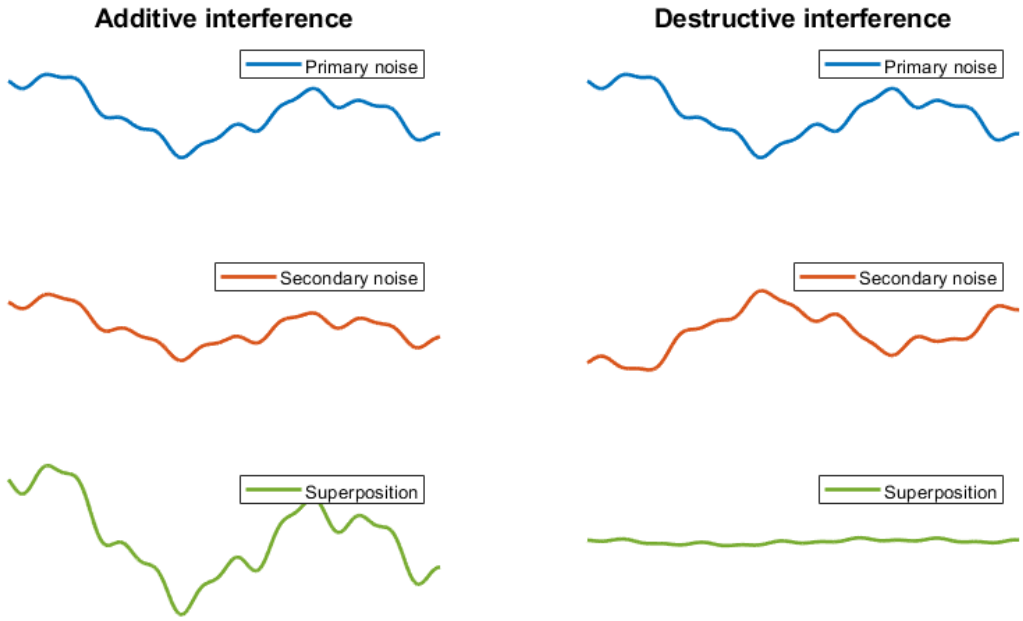

(a) Additive interference (b) Destructive interference

Figure 1: Examples of additive and destructive interference.

in practice, though. Given a primary noise signal d, the anti-noise signal y must very closely match the desired amplitude and phase – even small deteriorations in either of those quickly reduce the achieved attenuation. As a rule of thumb, when considering sinusoidal signals, maximum of about $\Delta\phi = 20°$ phase error can be tolerated to achieve sound attenuation of 10 dB, if the magnitude of the primary noise is matched perfectly [23]. The breakout point between destructive and additive interference is at $\Delta\phi = 60°$ phase error – if the error is higher than this, the anti-noise amplifies the primary sound instead of attenuating it. Figure 2 demonstrates how different magnitudes of error between desired and realized phase and amplitude affect the achieved noise attenuation.

Another important aspect to note is that active noise control is more difficult at higher than it is at lower frequencies. As the wavelength is shorter at higher frequencies – recall that wavelength is calculated as $\lambda = c/f$, where c is the speed of sound and f is frequency – a phase shift of $\Delta\phi$ degrees corresponds to a smaller dislocation in time Δt than at the lower frequencies. This means that the same temporal error in the anti-noise signal leads to larger error in phase with higher than with lower frequencies. Figure 3 shows the relation between temporal error in milliseconds and phase error in degrees at different frequencies, and in conjunction with Figure 2 shows how much the temporal error in anti-noise deteriorates the performance of ANC at different frequencies.

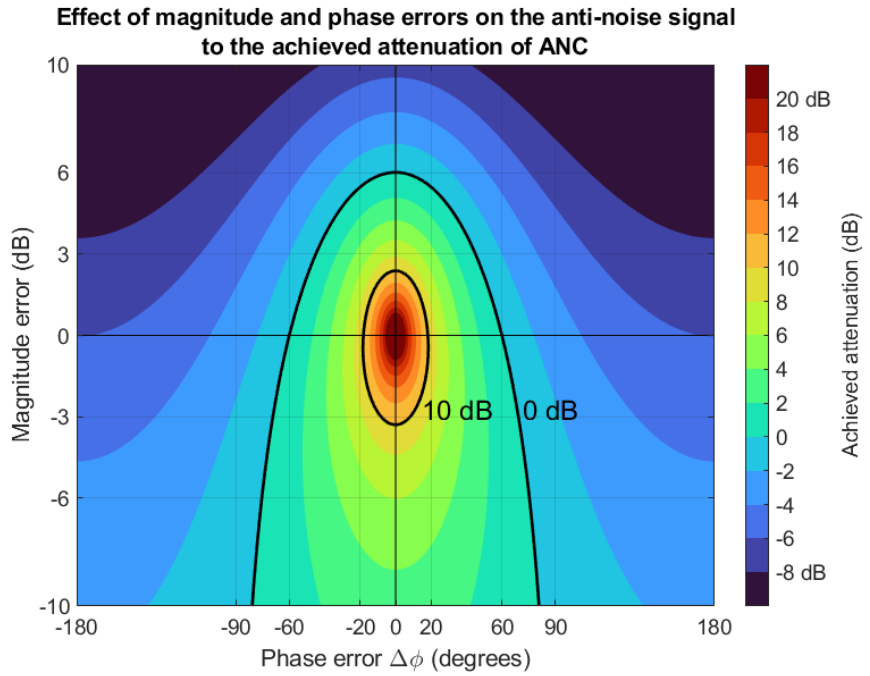

Figure 2: Effect of phase and magnitude errors to the resulting noise attenuation when considering pure sinusoidal signals. Both variables are presented relative to the ideal anti-noise signal. In addition, curves corresponding to 0 dB and 10 dB attenuations are presented. (Based on [25].)

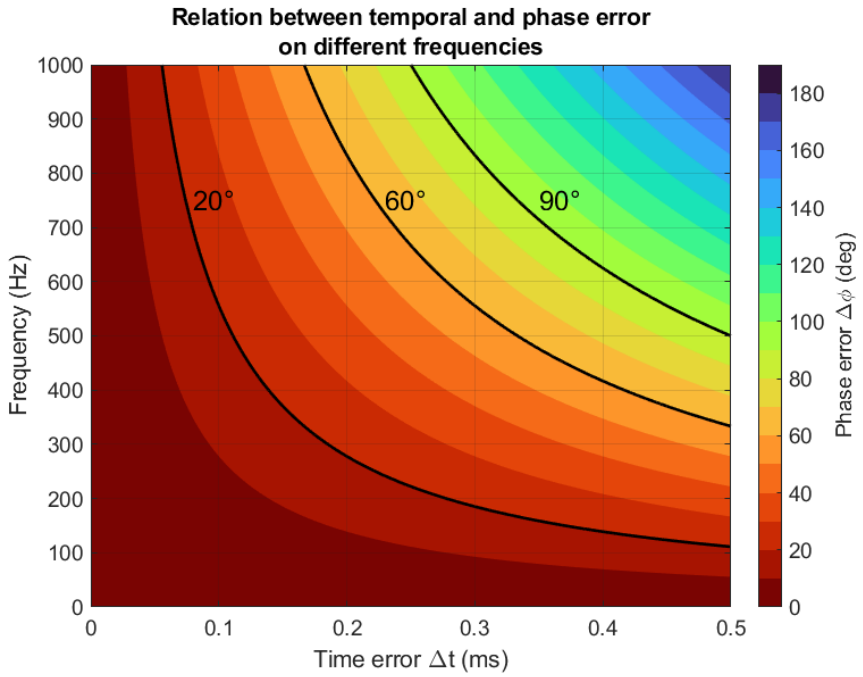

Figure 3: Relation between temporal (time) difference to the corresponding phase difference of two sinusoidal signals, on different frequencies.

2.3 Feed-forward ANC

The first major division between different control schemes is between feed-forward and feedback ANC. Feed-forward control incorporates one or more *reference sensors*, typically microphones, which are located close to the noise source. This way the controller gets to know the incoming primary noise ahead of time and has enough time to calculate and produce the needed anti-noise signal before primary noise reaches the measurement location. This signal is known as *reference signal* and is denoted by x. In addition to the reference sensor, the system includes a secondary source responsible of producing the anti-noise signal, an error sensor measuring the residual signal in the measurement location, and a controller controlling the different devices and producing the anti-noise signal. An example of a feed-forward ANC system in an air duct is shown in Figure 4.

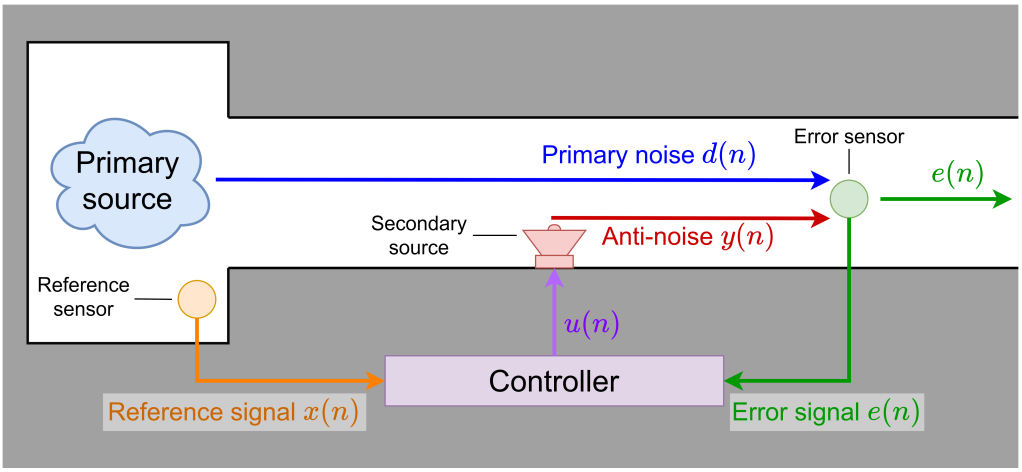

Figure 4: An example of a feed-forward ANC system in a ventilation duct.

The idea behind digital feed-forward control goes as follows. First, a reference sensor is placed close to the primary noise source to get a reference signal $x(n)$. This signal then travels through a primary path $P(z)$, representing the acoustic path from the reference sensor to the error sensor. The reference signal x filtered with the primary path P is called *primary noise*, and is denoted by $d(n)$. To produce the anti-noise, the reference signal x is modified by the controller $H(z)$, resulting in filtered signal $u(n)$. The signal u then goes through a *secondary path* $S(z)$ resulting in the anti-noise signal $y(n)$. The secondary path S represents all stages between the controller output and error microphone output: time delay needed to process the signal, digital-to-analog conversion, loudspeaker response, acoustic path from secondary source to error microphone, error microphone response, and analog-to-digital conversion [5]. Finally, the error signal, often also called residual signal, $e(n)$ is the acoustic pressure captured by error microphone, which is equivalent to the superposition of the primary noise and anti-noise signals: $e(n) = d(n) + y(n)$. Based on the resulting error signal, the controller modifies its response $H(z)$ suitably with some adaptive algorithm to minimize the error signal. A block diagram of the system shown in Figure 4 can be seen in Figure 5.

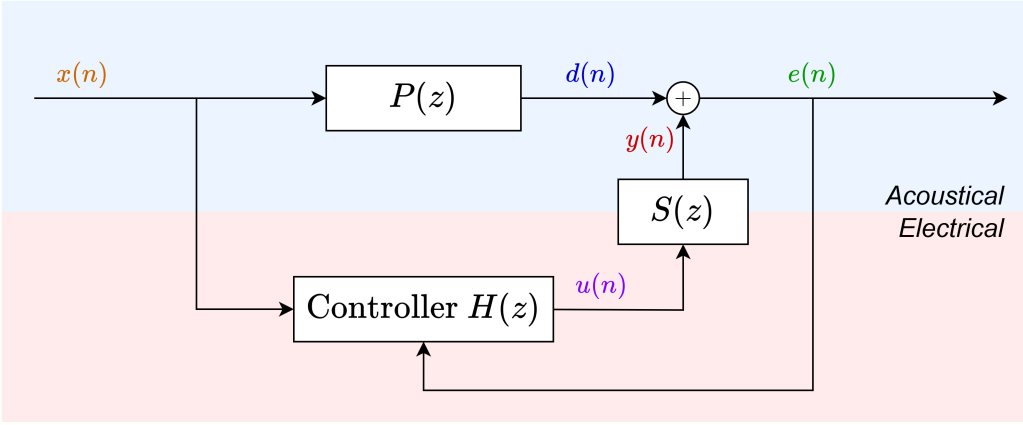

Figure 5: Block diagram of the feed-forward ANC system shown in Figure 4.

Assuming a linear time-invariant system, the relations between different signals can be derived with the help of Figure 5. The primary noise is equal to the reference signal filtered with the primary path impulse response:

$$D(z) = P(z)X(z). \tag{2}$$

Anti-noise signal $y(n)$, on the other hand, is equal to the reference signal $x(n)$ filtered by both the controller response H and secondary path response S:

$$Y(z) = H(z)S(z)X(z) \tag{3}$$

The residual signal $e(n)$ is the superposition of these two signals. In the desired outcome, this residual is zero; thus,

$$\begin{aligned} E(z) &= D(z) + Y(z) \\ &= P(z)X(z) + H(z)S(z)X(z) \\ &= 0 \\ \longrightarrow H(z) &= -\frac{P(z)}{S(z)}. \end{aligned} \tag{4}$$

In other words, when $X \neq 0$, the controller H tries at the same time to model both the primary path response $P(z)$ and the inverse of secondary path response $S(z)$. Therefore, feed-forward ANC is essentially a system identifying problem: the system has to identify responses of P and S to be able to accurately modify x into d [5]. It's not practical to use a controller H with a fixed response even if the responses of P and S would somehow be exactly known, as those responses are subjected to change over time. This can happen due to e.g. speed of sound slightly changing due to changes in temperature, or aging of components leading to microphone or loudspeaker responses slowly to shift. As seen earlier, even small differences in the desired and realized phase and amplitude of the anti-noise can severely affect the attenuation capabilities of the system, and thus, the controller typically uses adaptive filters

in their design. An adaptive filter's weights W are iteratively updated according to some algorithm to minimize some error quantity, such as the expected acoustic pressure measured with the error microphone. Many adaptive techniques have been developed for the purposes of active noise control, and these are the focus of Chapter 3. For the remainder of this chapter, it is sufficient to simply assume that there exists some algorithm which suitably modifies the response H to minimize the error signal e.

If certain conditions are met, a feed-forward ANC system is able to cancel out both broadband and narrowband noise. There are some potential issues, though, which must be taken into account when implementing the system. If the time delay of P is smaller than time delay of S, the performance of the system severely degrades. Intuitively, this situation would mean that the primary noise would reach the error sensor before anti-noise does, making the ideal controller response H non-causal [5]. If the causality condition is met – the controller has enough time to produce the anti-noise signal – the system is able to cancel out broadband noise; if it is not, the system is able to only cancel out narrowband noise [5]. Another potential issue of feed-forward systems is that the anti-noise signal y typically also propagates upstream towards reference sensor, corrupting the clean reference signal [5], though there are ways to mitigate this effect [26].

A fundamental requirement of a feed-forward ANC system is the availability of a coherent reference signal, which is correlated with the primary noise signal and which simultaneously satisfies the causality constraint of the system, or multiple such reference signals in the case of multi-channel feed-forward ANC. If such a signal is not available, the feed-forward system effectively reduces into a feedback system, being only able to cancel out narrowband noise. This can be the case in 2D- or 3D-cases where a sound is coming from opposite direction of the reference sensor relative to the error sensor, or in general if the sound field is diffuse. Therefore, careful planning must be made when creating a feed-forward ANC system into 2D- or 3D-spaces. Typically, these systems are multi-channel ANC systems with multiple in- and outputs.

Even with these limitations, feed-forward systems are used in multiple applications, as they tend to be more robust than feedback systems [26]. Compared to feedback control introduced later, feed-forward control has improved sound attenuation and stability. Aside from the air ducts presented earlier, feed-forward systems are under active research and are used in e.g. active noise cancelling headphones [14] as well as inside aircraft [18] and car cabins [27].

2.4 Feedback ANC

In contrast to feed-forward systems, feedback ANC systems do not incorporate a reference sensor, and in their simplest form only include an error microphone, a secondary source, and a controller generating the anti-noise. An example of such a system in a ventilation duct is shown in Figure 6, and its block diagram is shown in Figure 7. This system is simple in physical architecture, but not having the reference signal available limits the system performance. The most obvious limitation is that

the controller does not have any information about the primary noise other than the resulting residual signal, which directly implicates that a feedback ANC system is only able to control sound that it is able to predict based on the previous samples of the primary noise.

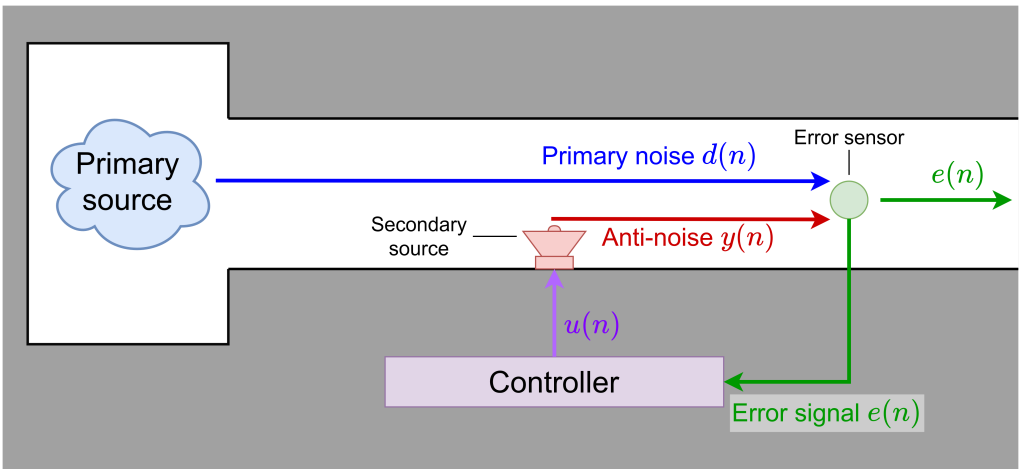

Figure 6: An example of a feedback ANC system in a ventilation duct; cf. Figure 4.

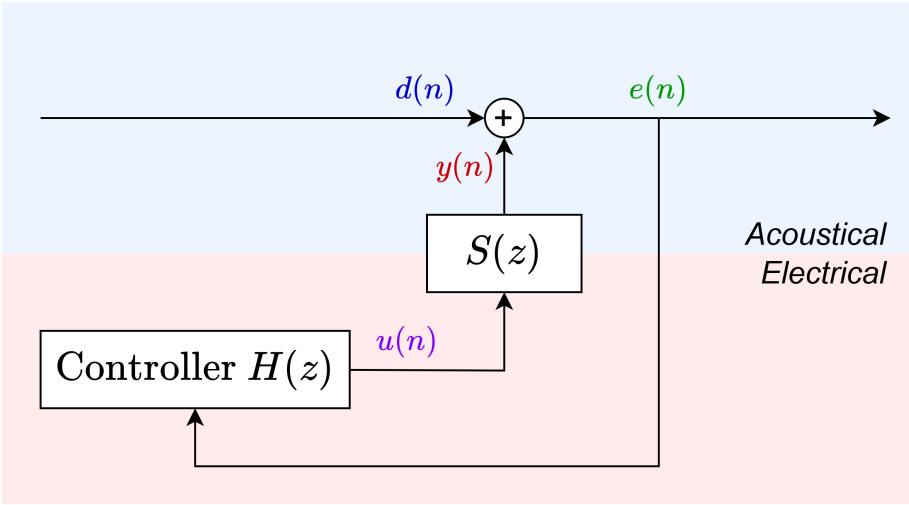

Figure 7: Block diagram of the feedback ANC system shown in Figure 6.

Whereas the feed-forward controller could be described as a system identification problem – find P and S such that reference signal x can be transformed into $y(n) = -d(n)$ – feedback controller can be described as a prediction problem: based on last N samples of d, predict next samples of d. This is possible with periodic signals and to some extent on other narrowband signals as well, but impossible with random signals, such as with white noise. It is also intuitive that it is more difficult to predict samples longer into future than it is only for a couple of samples ahead. Thus, the time delay imposed by S, Δ_S, plays a crucial role in the performance of a feedback ANC system. In addition to the causality problem, special care has to

be taken to ensure that the system will be stable, as with all feedback systems. For example, errors in the controller phase response can change the desired negative feedback into a positive one, resulting in oscillations [26].

In short, feedback ANC systems can control predictable sound or predictable components of the sound, which in essence means narrowband noise. Conversely, they are not able to control unpredictable sound, such as broadband noise or sudden, unexpected changes in the signal. Still, feedback ANC is the only viable solution in cases where there are no clean reference signals available, which can be the case for example in a room, where the sound field is diffuse or it is otherwise impractical or impossible to determine the direction where the sound is coming from. In addition, feedback control is used in environments where the latency induced by the secondary path is very short, such as in active noise cancelling headphones, either by itself or in conjunction with feed-forward control [28]. If the secondary path latency is very short, the performance of feedback system can even exceed that of a feed-forward one [29].

2.5 Global ANC

Global ANC means the approach that the noise of an entire large space, such as a room or a car, is attenuated with active noise control, in which case the quantity to be minimized is typically the acoustic potential energy in the controlled area [30]. Active control in a 3D-space is as its most effective close to the noise source. In particular, if the secondary source(s) can be placed close to the noise source, relative to the acoustic wavelength, active control can in fact decrease the total power output of the combined primary noise and secondary noise sources [22], [23]. This can be practical, for example, in a situation where a loud machine is fixed to a certain place in an industrial plant. However, it is impractical in situations where the primary noise source cannot directly be accessed or if its location varies.

One issue of global ANC is that measuring the acoustic potential energy in the room requires large arrays of microphones whose spacing is dependent on the wavelength of the sound [30]; thus, the complexity of the system is dependent on both the enclosure size and the maximum primary noise frequency. An intuitive approach to attenuate total acoustic energy in an enclosure would be to somehow replicate the inverse of the complete sound field inside the said enclosure, thus negating the total acoustic pressure by superposition principle. By Huygens' principle, assuming that all primary sound sources lie outside the enclosure, the resulting sound field can be exactly replicated with a suitable arrangement of secondary sources in the enclosure boundary [31]. This theoretical result has severe practical limitations, however, as the number of needed reference sensors and secondary sources becomes unreasonably large even for quite low frequencies [30]. Also, this kind of system would not be able to attenuate noise whose origin is inside the enclosure due to the controller becoming non-causal.

Another way of achieving global ANC is by attenuating some individual room modes with a secondary source instead of trying to replicate the whole sound field [32]. This method can achieve reduction of the total acoustic potential energy in

the room [23], but is only useful for frequencies whose modal density is low, i.e. the sound field is not diffuse. In principle, the number of secondary sources needed to perfectly cancel sound in an enclosure is the same as the number of acoustic modes being excited [26]; and as the modal density increases with frequency, global noise control is particularly difficult at high frequencies. The transition from low to high modal density range is usually defined with the Schroeder frequency, calculated with $f_{Sch} = 3.91/T_{60}$, where T_{60} is the reverberation time of the room [33]. As the reverberation time typically increases with the room size, the upper frequency limit of global ANC with room mode suppression decreases as the room size increases. Additionally, these systems must be carefully designed to the space in question [32], and expensive and time-consuming calibration must be made after relocating the system [30].

2.6 Local ANC

Whereas global ANC systems try to minimize sound in a whole room, local ANC systems only focus on a single point, or multiple discrete points in space. Local ANC systems create a *zone of quiet* around the error microphone. The radius of this spherical area varies as a function of wavelength: the higher the frequency, the smaller the area. As a rule of thumb, 10 dB attenuation of the primary noise is achievable in a spherical area with diameter of about 1/10th of the wavelength [23]. For 100 Hz tonal noise this diameter is equivalent to about 30 cm, whereas for 1 kHz tonal noise the diameter is reduced to about 3 cm.

Local ANC attenuates the sound level at the error microphone, but placing a physical device to the desired place is not always practical or possible; for example, zones of quiet should be located near the user's ears, but holding microphones very near one's head is practically as restrictive as wearing proper hearing protection [34]. Thus, different virtual sensing techniques have been developed, where the sound pressure level of a remote position is estimated using one or multiple physical microphones located nearby. The simplest technique is to measure the transfer function from the physical microphone(s) to the virtual microphones located at the ears beforehand, but this method is sensitive to head movement, as the virtual microphones are not moved along the head. A better way is to use a multiple-microphone setup, where the virtual microphones are placed by tracking the head placement with some external method and the sound level at that remote position is extrapolated from the difference of two physical microphones [34].

As a local ANC system does not know nor care about the sound pressure in points other than at the microphone locations, it is inevitable that the sound pressure level is actually increased at some points, as the total sound power radiated into the room is increased due to the secondary source. The goal of designing local ANC systems is thus to maximize the size of the zone of quiet while simultaneously minimizing the increased sound pressure level outside the zone of quiet.

While in principle global control is often more desirable – attenuate the whole room instead of just a single point in it – local ANC has been researched more extensively and has gained more popularity due to it being simpler to achieve. In

addition, local active noise control systems can achieve larger attenuation, albeit only in close proximity of the error sensor.

2.7 Spatial ANC

Spatial ANC can be seen as the intermediate step between global and local ANC. If multiple microphones are arranged into a circular or spherical array, local ANC can achieve major attenuation in the microphone locations, but the attenuation is guaranteed only at those discrete points. The sound pressure is not guaranteed to reduce between two microphones or at an arbitrary point inside the array, and at some points the acoustic pressure will be even higher than what it would be without using the ANC system.

The goal of spatial ANC systems is to control the whole sound field over some spatial area, with the quantity to be minimized being, for example, total acoustic potential energy inside a loudspeaker array. A fundamental problem is that the acoustic pressure at other points than those at which the microphones are located cannot be directly measured. Spatial ANC systems overcome this issue by representing the whole sound field inside the array based on the finite number of measured signals. For example, Zhang's doctoral dissertation [35] researched wave-domain signal processing, which essentially means decomposing the controlled sound field into spherical harmonics and controlling the weights of these basis sound fields. As wave-domain signal processing controls the whole propagating sound field rather than a set of discrete points, it is more effective on controlling noise over large area [35].

Despite their apparent potential, such spatial ANC systems have not yet been realized as commercial products. One reason is their complexity: to achieve spatial noise reduction, large arrays of microphones and loudspeakers have to be used. For example, the research in [15] used a circular array of 11 microphones and loudspeakers in 2D-simulations. They also tried the same simulations with 9, 7 or 5 loudspeakers, but the results were significantly poorer [15]. On the other hand, [16] used a "2.5D" approach in a 3D-space with a single circular loudspeaker array of 11 loudspeakers, which, while having significantly less components than a complete spherical loudspeaker array would have, still has quite many components for a commercial use, if the system is often required to be relocated to another place.

Figure 8 summarizes the difference between global, local and spatial ANC systems' effective areas.

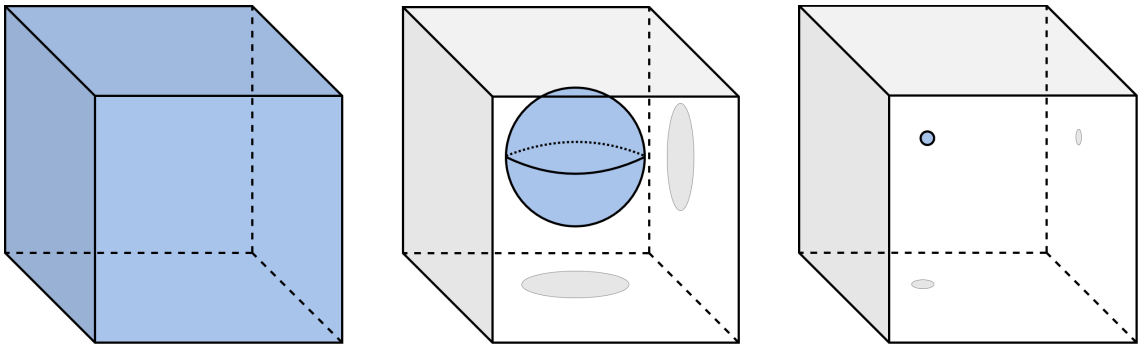

(a) Global ANC (b) Spatial ANC (c) Local ANC

Figure 8: Three different design principles for ANC systems' effective area: global, spatial, and local control.

3 Adaptive algorithms in active noise control

The different ANC system structures introduced in previous chapter included the controller $H(z)$ as a black box – it was simply assumed that there exists an algorithm which suitably modifies the reference or error signal to accurately produce the needed anti-noise. In practice, these algorithms usually incorporate one or multiple finite impulse response (FIR) filters whose weights are updated according to some rule, though this is not the only way to conduct ANC.

The main problem of the adaptive filtering can be formulated by iteratively finding the optimal filter weights $\mathbf{w}(n)$ for the adaptive filter $W(z)$ which mimimize some cost function or an error quantity. There are multiple approaches to this, but the most commonly used algorithms are based on the least mean squares (LMS) algorithm due to its simplicity and effectiveness. As such, this thesis focuses on these algorithms.

Rest of this chapter introduces different adaptive filtering structures and other issues that must be taken into account in active noise control. First, the LMS algorithm is explained, after which some well-known improvements and modifications to the basic LMS algorithm are introduced. These algorithms form the backbone of ANC systems. Finally, one non-linear and one discrete wavelet transform based algorithms are introduced.

3.1 Least mean squares (LMS)

In its core, least mean squares algorithm (LMS, also known as stochastic gradient algorithm [26]) has been available for over half a century [20], [21]. It is quite a simple gradient descent algorithm based on minimizing the error signal's mean squared error, and forms the basis of many other adaptive algorithms. Figure 9 shows block diagram of LMS applied to an ANC system.

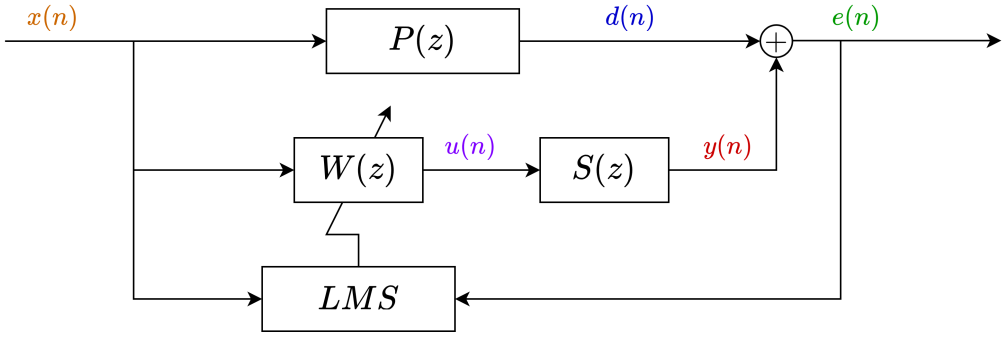

Figure 9: Block diagram of the LMS algorithm.

Denote the expected mean square error of e by ξ:

$$\xi(n) := \mathbb{E}[e^2(n)], \tag{5}$$

where e is the error signal and $\mathbb{E}$ is the expected value operator [26]. This value $\xi(n)$ acts as the cost function J of the algorithm,

$$J_{LMS}(n) := \xi(n). \tag{6}$$

This means that the algorithm aims to minimize the expected value of squared error signal. This is done by iteratively updating adaptive filter coefficients $\mathbf{w}(n) = [w_0(n), w_1(n) \dots w_{L-1}(n)]^T$, where L is the filter length and ^{T} denotes transpose operation, into negative direction of the gradient of ξ w.r.t. filter weights $\mathbf{w}$. By doing this, the weights travel step by step towards the global minimum of this gradient [26]; thus,

$$\mathbf{w}(n+1) = \mathbf{w}(n) - \mu\nabla\xi(n), \tag{7}$$

where μ is a constant *step size* or *learning factor* of the algorithm. However, $\xi(n)$ cannot be directly computed without knowing more about the stochastic behaviour of x. This issue is solved by estimating the gradient of $\xi(n)$ with

$$\nabla\hat{\xi}(n) = -2\mathbf{x}(n)e(n), \tag{8}$$

where $\mathbf{x}(n) = [x(n), x(n-1), x(n-2) \dots x(n-L+1)]^T$ is a vector containing the last L samples of the reference signal. This finally results to the weight update rule used in LMS:

$$\mathbf{w}(n+1) = \mathbf{w}(n) + \mu e(n)\mathbf{x}(n). \tag{9}$$

Note that in some literature, such as in [22], the right hand side of the equation 9 uses 2μ in place of μ, mainly due to the factor of 2 conveniently carrying on from the derivation of the equation. However, it makes no practical difference whether the equation contains the factor 2 or not, as one could always choose double or half the value for μ to end up to the same result; thus, the factor 2 is omitted in this thesis, and all other equations are adjusted accordingly.

The convergence of basic LMS algorithm is dependent on the step size μ. However, there is no universal single best value for it; rather, the suitable choice for μ depends on the statistics of the reference signal $x(n)$, or more specifically, how correlated it is. LMS is proved to converge if and only if

$$0 < \mu < \frac{2}{\lambda_{max}}, \tag{10}$$

where λ_{max} is the largest eigenvalue of autocorrelation matrix of $\mathbf{x}$ [22], [26]; in fact, it is shown that fastest convergence is achieved when $\mu = 1/\lambda_{max}$ [26]. However, calculating the autocorrelation matrix at each time step is a high computational burden if L is large. Therefore, a suitable value for μ has to be estimated by some suitable method.

The other parameter in LMS is the adaptive filter length L. Recall from Section 2.3 that the controller H, or in this case the adaptive filter W, tries to simultaneously

model the primary path P and inverse of the secondary path S:

$$W(z) = -\frac{P(z)}{S(z)}. \tag{11}$$

Thus, the number of filter coefficients must be chosen so that it can model the impulse response accurately enough, when considering broadband signals [26]; and when considering narrowband signals, the impulse response $\mathbf{w}(n)$ must include a sufficient portion of the primary noise signal's period [26]. On the other hand, choosing a too long filter unnecessarily increases the computational cost.

LMS is mainly used due to its simplicity and model-independent performance, but its performance is limited by relatively slow convergence [36]. While LMS is relatively robust in system identification and signal estimation, it has several drawbacks when used in active noise control, which are explained and solutions to them introduced in the following sections.

3.2 Normalized LMS (NLMS)

The performance of LMS algorithm is only controlled by the chosen step size, but is also dependent on the reference signal's power (and with that, indirectly by the filter length L) [26]; thus, with the same μ, signals with larger power converge more quickly than those with smaller power, which is typically undesired behaviour. What is even worse is that the convergence might be optimal for some signal levels but unstable for higher. One technique of making the suitable choice of μ independent of the reference signal's power is to normalize the step size with the reference signal's power. This is known as the *normalized least mean squares* algorithm (NLMS). In NLMS the weights are updated with [26]

$$\mathbf{w}(n+1) = \mathbf{w}(n) + \mu(n)e(n)\mathbf{x}(n), \tag{12}$$

where $\mu(n)$ is computed with

$$\mu(n) = \frac{\alpha}{\beta + \mathbf{x}(n)^T\mathbf{x}(n)}, \tag{13}$$

where α is a normalized step size satisfying $0 < \alpha < 2$, β is a small constant ensuring that the denominator is not too small in case of reference signal having small power, and $\mathbf{x}$ is a column vector containing last L samples of reference signal x.

3.3 Feed-forward filtered-x LMS (FxLMS)

Figure 9 showed the block diagram of the LMS algorithm applied to an ANC system. In a practical, real-life environment, the secondary path S always induces a phase shift to the adaptive filter output u, which leads to $x(n)$ and $e(n)$ being out of phase relative to each other. In practice this means that the reference signal $\mathbf{x}$ and error signal e do not correspond to each other in gradient estimate calculation in equation 8, and thus, the gradient estimate in by itself is not accurate. The LMS algorithm can

tolerate this to some extent, but if the phase error increases too high, the algorithm starts to diverge.

Filtered-reference LMS, commonly also known as *filtered-x LMS* (FxLMS) due to reference signal often denoted by x, solves this issue by filtering the reference signal x with an estimate of the secondary path $\hat{S}$ creating a *secondary-path filtered reference signal* $\hat{x}$, which is then fed to the LMS algorithm. Assuming perfect estimation $\hat{S} = S$, both the reference and error signals fed to LMS are now filtered with the same filter, and are thus aligned in time. A block diagram of the FxLMS algorithm is seen in Figure 10.

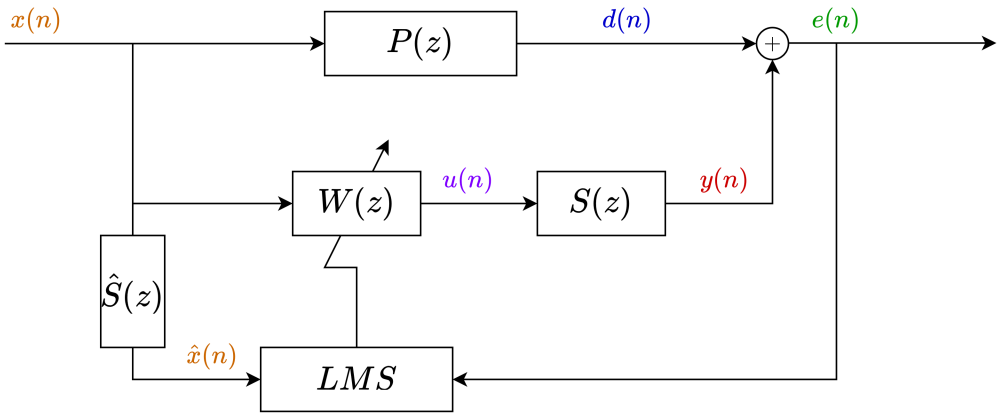

Figure 10: Block diagram of the FxLMS algorithm.

For the update rule, FxLMS simply replaces the reference signal x with its filtered counterpart $\hat{x}$. Therefore, the update rule for the basic FxLMS is [22], [26]

$$\mathbf{w}(n+1) = \mathbf{w}(n) + \mu e(n)\hat{\mathbf{x}}(n), \tag{14}$$

and for the normalized FxLMS (NFxLMS)

$$\begin{aligned} \mathbf{w}(n+1) &= \mathbf{w}(n) + \mu(n)e(n)\hat{\mathbf{x}}(n) \\ &= \mathbf{w}(n) + \frac{\alpha e(n)\hat{\mathbf{x}}(n)}{\beta + \hat{\mathbf{x}}(n)^T\hat{\mathbf{x}}(n)}. \end{aligned} \tag{15}$$

The maximum step size that can be used with FxLMS is approximately

$$\mu_{max} = \frac{1}{\sigma_{\hat{x}}(L + \Delta_S)}, \tag{16}$$

where $\sigma_{\hat{x}}$ is the power of the filtered reference signal and Δ_S is the total time delay in samples caused by the secondary path [26]. When applied to normalized FxLMS, this corresponds to approximately

$$\alpha_{max} = \frac{1}{L + \Delta_S}, \tag{17}$$

provided that the constant β in equation 13 is small. Therefore, the length of the secondary path severely limits the step size and therefore convergence of the FxLMS

algorithm, even if the secondary path would be estimated perfectly; however, it has been found that the time delay Δ_S has only minor effect on the steady-state performance of the system [26].

In any practical setting, $\hat{S} \neq S$. FxLMS is robust against this imperfection, and phase errors up to 40° hardly affect the convergence speed [26]; however, the estimate has to match the real response's phase within 90° in all frequencies for it to remain stable [22], [26]. Even if the phase error is under 90°, though, larger errors on the estimation leads to slower convergence or worse steady state performance [22], [26], and therefore, an estimate with high precision is desired.

The secondary path estimation can be acquired either by measuring the secondary path response before operating the system, or during its operation. The former is called *offline estimation* and is simpler, but as the response is measured just once, the system won't be able to track changes in the actual response, which could become an issue if the response is time-varying [26]. The other approach is to estimate the secondary path during the ANC operation, called *online estimation*, typically performed by injecting white noise to the anti-noise signal [26], [37]. However, the various secondary path estimation techniques are not in the focus of this thesis.

3.4 Leaky FxLMS (LFxLMS)

LMS only attempts to minimize the mean square value of the error signal [22], which leaves the weights of the adaptive filter unconstrained. One modification to this is to use the weighted sum of the mean square value of the error signal and the sum of the filter weights as a cost function. Thus, the cost function under subject of minimization would be

$$J_{LLMS} = \xi(n) + \gamma \mathbf{w}^T \mathbf{w}, \tag{18}$$

where γ is a *leaky factor*, $\gamma > 0$, and $\mathbf{w}$ is a column vector of adaptive filter weights [22]. Using the same approximation for $\nabla\xi(n)$ as earlier, the update rule becomes

$$\mathbf{w}(n+1) = (1 - \gamma\mu)\mathbf{w}(n) + \mu e(n)\mathbf{x}(n). \tag{19}$$

This algorithm is called leaky LMS due to the term $(1 - \gamma\mu)$, which "leaks" $\mathbf{w}$ away in case the error signal is zero [22]. The leaking term can be applied also to FxLMS, in which case the update rule becomes

$$\mathbf{w}(n+1) = (1 - \gamma\mu)\mathbf{w}(n) + \mu e(n)\hat{\mathbf{x}}(n), \tag{20}$$

and to normalized FxLMS, in which case the update rule is

$$\begin{aligned} \mathbf{w}(n+1) &= (1 - \gamma\mu)\mathbf{w}(n) + \mu(n)e(n)\hat{\mathbf{x}}(n) \\ &= (1 - \gamma\mu)\mathbf{w}(n) + \frac{\alpha\mu e(n)\hat{\mathbf{x}}(n)}{\beta + \hat{\mathbf{x}}(n)^T\hat{\mathbf{x}}(n)}. \end{aligned} \tag{21}$$

Using leaky FxLMS over normal FxLMS makes the convergence more robust, but introducing the leaking term inevitably degrades the attenuation of the system

[22]. However, a small γ can in many applications significantly improve the stability with only small degradation in the maximum attenuation [22].

3.5 Internal model control (IMC)

The algorithms presented thus far have all been designed for feed-forward control, as they all need a reference signal x. However, the feedback system shown in Section 2.4 in Figure 7 can be transformed into an equivalent feed-forward one, after which the previously shown algorithms can be applied. The block diagram of this *internal model control* (IMC) system can be seen in Figure 11.

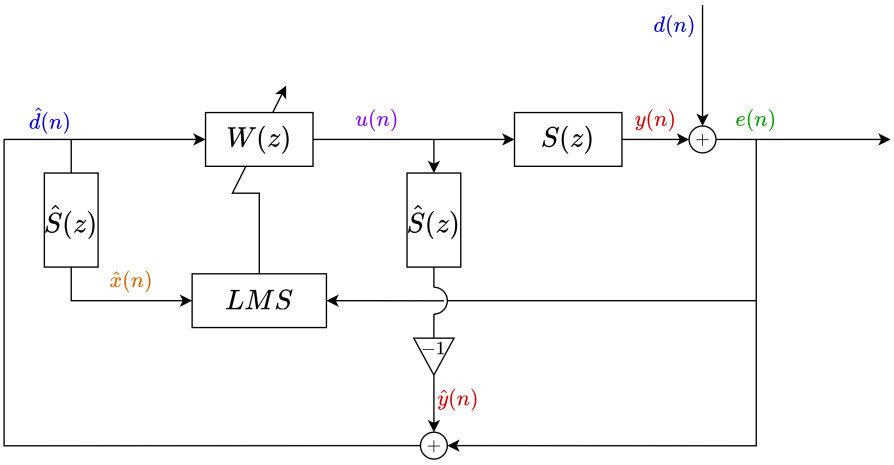

Figure 11: Block diagram of the FxLMS algorithm with internal model control.

Once again, the anti-noise signal y is produced by the adaptive filter output signal u going through the secondary path, and the error signal e is the sum of primary noise d and anti-noise y:

$$\begin{aligned} Y(z) &= S(z)U(z) \\ E(z) &= D(z) + Y(z) \\ &= D(z) + S(z)U(z). \end{aligned} \tag{22}$$

Using an estimate $\hat{S}$ of the secondary path S, the system then internally calculates a model $\hat{y}$ of the anti-noise signal y (hence the name):

$$\hat{Y}(z) = \hat{S}(z)U(z). \tag{23}$$

Finally, the system calculates a synthesized reference signal $\hat{d}$ by subtracting the anti-noise estimation from the error signal:

$$\begin{aligned} \hat{D}(z) &= E(z) - \hat{Y}(z) \\ &= D(z) + S(z)U(z) - \hat{S}(z)U(z) \\ &= D(z) + U(z)\left[S(z) - \hat{S}(z)\right]. \end{aligned} \tag{24}$$

If the model of the secondary path is perfect, $\hat{S} = S$, then also $\hat{D} = D$ by equation 24. It has been shown that in this case, the system is internally stable: any bounded input yields a bounded output [22]. However, once again the model is never perfect. Figure 12 shows the IMC system from Figure 11 rearranged. From that it can be seen that the modeling error $S - \hat{S}$ creates a feedback loop in the system, whose gain can be written as

$$H(z) = \left[S(z) - \hat{S}(z)\right] W(z). \tag{25}$$

If this loop has gain of less than unity on all frequencies, the modeling error has little impact on the convergence of the adaptive filter [22]. However, even with a very good but not perfect secondary path model, the gain could exceed unity on some frequencies, if the gain of the adaptive filter W is very large [22]. Thus, special care must be made to ensure that said gain does not become too large. One possible solution to this potential issue is to introduce a leakage term to the controller, as in leaky LMS.

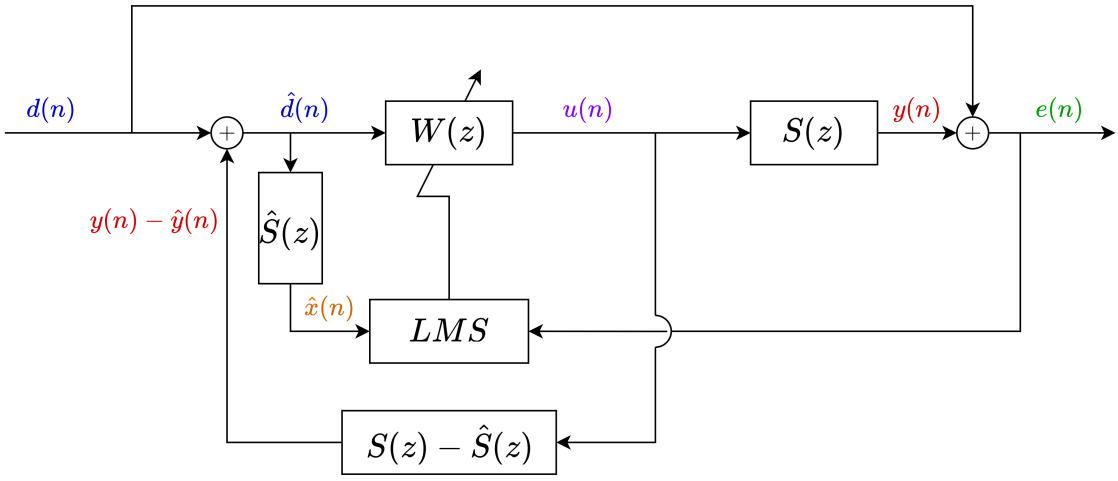

Figure 12: Block diagram shown in Figure 11 restructured. (Based on [26].)

Even if this system resembles the previously introduced feed-forward ones, especially when rearranged into the form shown in Figure 12, the causality problem explained previously in the context of feed-forward systems persists. Recall from Section 2.3 that for a feed-forward ANC system to be causal, the time delay of primary path P must be greater than the combined time of processing delay and the time delay of S; however, it can be interpreted from Figure 12 that in this system $P(z) = 1$, meaning that such condition can never be satisfied. This means that the system cannot produce the anti-noise beforehand and must predict the upcoming primary noise samples based on the past samples instead. In steady, periodic signals, this is not an issue. However, as the latency Δ_S of the secondary path increases, it becomes increasingly difficult to track the changes on even lower frequencies.

3.6 Feedback functional link artificial neural network based ANC (FLANN)

The previous sections have introduced the LMS algorithm and its well-known derivatives. The last two sections of this chapter will introduce two lesser researched variants of the LMS and especially IMC algorithms, one non-linear and one discrete wavelet transform based algorithm.

In practical applications, the primary path P, the secondary path S, or even the primary noise d can be non-linear [38]. The linear ANC algorithms cannot in this case fully replicate the non-linear nature of the needed anti-noise signal, and thus, many non-linear ANC algorithms have been developed [38]. One of these, based on the functional link artificial neural network (FLANN), is presented in this section.

A feedback ANC system based on IMC employing a FLANN expansion was introduced in [39]. It was designed to be effective on chaotic noise, which in the paper referred to non-linearly deterministic noise [39]. The block diagram of the system introduced in [39] is shown in Figure 13. The Figure 13 shows only one LMS controller to avoid clutter, but the system is realized with each adaptive filter W having their own controller, potentially with varying parameters.

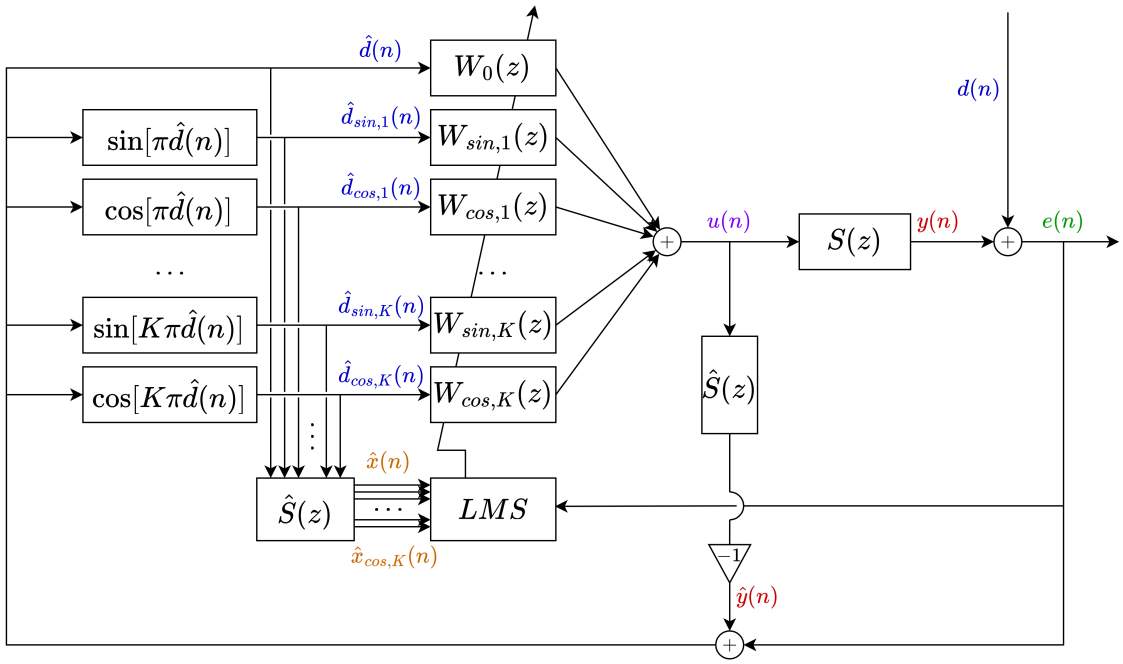

Figure 13: Block diagram of the FLANN-based feedback ANC algorithm of order K, introduced in [39].

Compared to the system introduced in Section 3.5, a non-linear trigonometric expansion of order K is conducted on the synthesized primary noise $\hat{d}$, after which both the original synthesized primary noise signal and the expanded components have their own adaptive filters and LMS controllers. Finally, the output of all these adaptive filters are combined, resulting in the control signal u.

The synthesized reference signal $\hat{d}$ is expanded into a sine and a cosine component for each order in the controller in addition to the unmodified signal $\hat{d}$; thus, the system consists of $2K + 1$ adaptive filters and LMS controllers, where K is the order of the controller. Each order of trigonometrically expanded signals can be calculated with

$$\begin{aligned} \hat{d}_{sin,k}(n) &= \sin\left[k\pi\hat{d}(n)\right], \\ \hat{d}_{cos,k}(n) &= \cos\left[k\pi\hat{d}(n)\right], \end{aligned} \tag{26}$$

where k is the order of the said path.

The algorithm was reported to outperform the conventional FxLMS algorithm [39], though the results showed in [39] only focused on chaotic noise.

3.7 Discrete wavelet packet transform based ANC

An feedback ANC algorithm based on wavelet packet transform was introduced in [40]. A block diagram of the said system can be seen in Figure 14.

Wavelet packet transform is a multi-resolution signal analysis technique for time-frequency domain analysis [40]. In essence, it decomposes the signal according to small wavelets, short quickly decaying oscillating waves, in contrast to the infinite sine waves used in Fourier transform. This is realized by filtering the signal with two complementary filters, a high-pass filter $A(z)$ and a low-pass filter $D(z)$. This is repeated for each signal component filtered such a way for each level, or order, of the controller; thus, the signal is decomposed into 2^K components, where K is the controller order. The weights of A and D are dependent on the used wavelet.

The structure seen in Figure 14 can also be seen as a subband ANC, where the signal is divided into frequency components and each component is controlled separately. The wavelet packet transform based ANC was reported to outperform traditional FxLMS on broadband noise cancellation in [40].

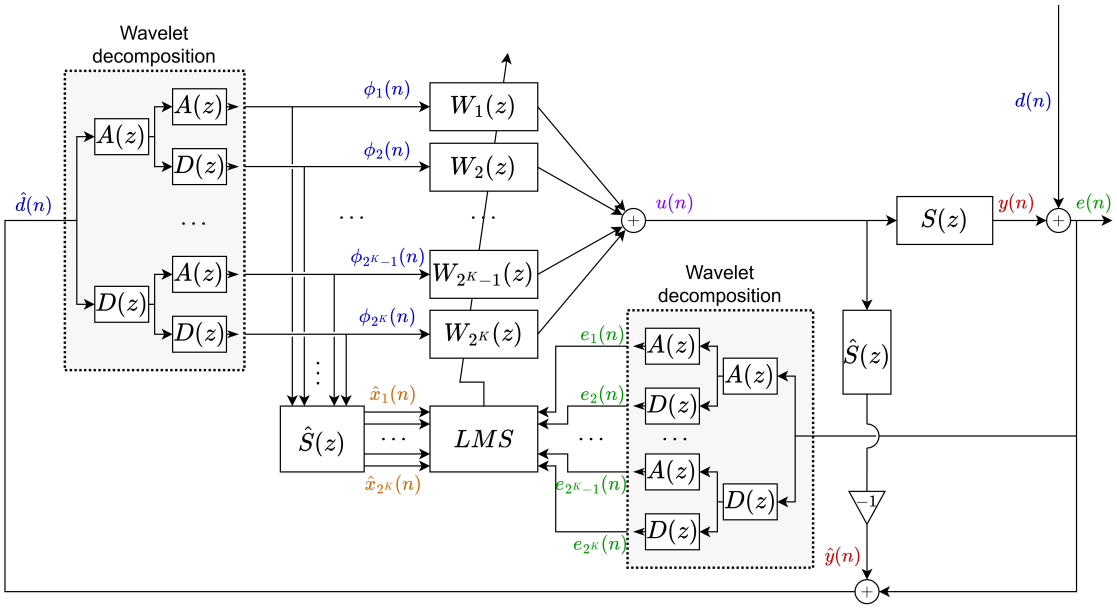

Figure 14: Block diagram of the wavelet packet decomposition based feedback ANC algorithm of order k, introduced in [40].

4 ANC system design

This chapter derives the main goals and design choices for the prototype ANC system briefly introduced in Chapter 1. First, the goals of the ANC system are reviewed, after which different architectural choices are presented and justified based on the theory explained in Chapters 2 and 3. Based on the choices introduced here, a simulation environment is built and introduced in the next chapter.

4.1 Goals of the prototype system

Keeping the thesis goals introduced in Chapter 1 in mind, the goals of the ANC system were as follows:

1. The system must be usable in real 3D-spaces.

The goal is to create a real, physical device. While simulations and measurements in an anechoic room are an essential part of the design process, the system must be tested at other places as well. Furthermore, the system must work in real-time.

2. The system must be simple to use.

While it has been shown that having a more complex design often leads to better noise attenuation, the idea behind the system is that it would be practically as easy to use as active noise canceling headphones. The goal is thus to develop a system which does not need to be configured and calibrated to each space separately; rather, it should be usable with no or only minor setup. This also implies that the system cannot include unpractical amounts of components.

3. The system must work on both narrowband and broadband signals.

The chosen algorithms must be able to control both narrowband and broadband signals. The system is simulated and tested with both kinds of signals.

4. The system attenuates the sound pressure level as much as possible at the error microphone.

Minimizing the sound pressure level at the error microphone is not the only way to conduct active noise control, and it might sometimes be desired to shape or equalize the error signal's spectrum instead rather than to attenuate all frequencies equally [41], [42]. However, minimizing measured SPL was chosen due to it being simple and objective to measure, and often being a good starting point even if it would not be the final goal. For simplicity, Z-weighted (unweighted) SPL is measured.

4.2 Control scheme

Despite the limitations of feedback control introduced in Section 2.4, **the system was still decided to incorporate feedback control**. This is due to feed-forward

control being difficult to implement in a 3D-space where the primary noise source can be in any direction, as in that case the reference microphones should also be placed to all directions from the secondary source for the controller to be causal, as explained in Section 2.3. In practice, large microphone arrays should be used, which directly contradicts the design goals, stating that the system should be easy to use without the need of placing extensive amounts of microphones to the room before using the system. If this constraint is not loosed, feedback control remains as the only viable solution, albeit its limitations.

It should be noted, though, that the system could in principle incorporate only one or a few of these reference microphones, which could then be placed to the most noisy directions at will to enhance the attenuation from those directions. This would in practice turn the control scheme into hybrid for those directions, and feedback for the others; however, this idea was not explored further in this thesis.

4.3 Effective area

Local ANC was chosen as the effective area of the system. This is largely for the same reasons that feedback control was chosen. Spatial ANC cannot be achieved with one loudspeaker and microphone, or even with a few of them, once again contradicting the need of the system to be quick and easy to deploy. Global ANC could in theory be applied, if the goal would be to suppress room modes. However, that would need the loudspeaker to be adjusted carefully to the right place in the room, reducing the easiness of use; on the other hand, the usefulness of the device would be severely decreasing as the room size increases, as explained in Section 2.5.

4.4 System structure

Based on the chosen control scheme and effective area, the system was chosen to simply consist of one secondary source loudspeaker and one error microphone. In practice, this means that if this system would be commercialized as it is, the user would need to have a microphone near their head to get the zone of quiet near their ears. As Section 2.6 briefly discussed, there are virtual sensing technologies which could be used to avoid a wearable microphone. Further examination of the topic was left out from this thesis, but virtual sensing techniques could possibly be used in a future version of the system. Still, to emulate having the error microphone near but not directly at the users' ears, one other microphone was added to the system setup.

4.4.1 ANC algorithm

Chapter 3 introduced adaptive filtering as a concept as well as some algorithms developed for adaptive filtering in ANC. As the best choice out of those is not self-evident, multiple algorithms were chosen to be included in the measurements. The set of algorithms-to-be-tested was chosen to include different types of algorithms. LFxLMS introduced in 3.4 with the feedback structure introduced in Section 3.5 was chosen due to its simplicity and for being well researched, FLANN-based algorithm

("FLANN") introduced in 3.6 to include a non-linear algorithm, and wavelet packet transform based algorithm ("Wavelet") introduced in 3.7 due to the apparently potential wavelet transform and subband approaches. Furthermore, as all the algorithms had multiple tunable parameters, each of the chosen algorithms was tested with different combinations of those parameters as well.

As feedback ANC is essentially a prediction problem, using some completely different machine learning or artificial intelligence based methods, such as training a neural network to predict the incoming primary noise, was briefly considered. However, researching and implementing this was not possible in the time frame allocated for this thesis project, and thus, those were not included into the final simulations nor prototype system measurements.

4.4.2 Secondary path estimation

Section 3.3 briefly introduced techniques to estimate the secondary path, either by online or offline methods. For simplicity, the secondary path was decided to be determined offline before the measurements. For simulation, this means simply using the same impulse response for secondary path S and its estimate $\hat{S}$. For the real-world measurements, impulse response from secondary source to the error microphone is computed before measurements with a sine sweep.

Even though a potential commercial device should repeatedly be estimating the secondary path response online during its operation due to potentially changing conditions, there already exist well-researched methods of doing this in feedback ANC systems [26], [37]. Therefore, measuring the response offline beforehand in the prototype system is justified.

4.5 Evaluation criteria of the system

As the performance of an ANC system relies on many factors, it is not self-evident to choose the metric on which to evaluate the system with. First, the performance of the LMS algorithm is governed by the step size μ, which always introduces a trade-off between convergence speed and the magnitude of the residual signal, but it depends on the application which of these two is more important to be minimized. Second, the system is bound to work better on some signals than others, and comparing these results against each other is not straight-forward. Third, local ANC systems attenuate the sound at the error microphone, but one might be more interested in how the sound field behaves at other points in the room.

However, calculating a single quantity as the performance index is convenient for comparing the different algorithms, even though it might not take all these factors into account. Therefore, the main evaluation metric of the system performance was decided to be the *equivalent level difference* between the primary noise and error signals: how much the equivalent noise level decreased when the ANC system was used, compared to when it was not. This value is calculated in decibels with

$$L_{eq} = 10 \log_{10} \left(\frac{\text{mean}(\mathbf{d}(n)^2)}{\text{mean}(\mathbf{e}(n)^2)} \right) \text{ [dB]}, \tag{27}$$

where $\mathbf{d}$ is the complete primary noise signal and $\mathbf{e}$ is the complete error signal, mean($\mathbf{x}(n)$) denotes the arithmetic mean of vector $\mathbf{x}(n)$, and $\mathbf{x}(n)^2$ denotes the vector $\mathbf{x}$ squared element-wise:

$$\mathbf{x}(n)^2 = [x_0^2, x_1^2 \dots x_{L-1}^2]. \tag{28}$$

This calculation is done to each test signal separately. Thus, the algorithms are compared to each other signal-wise, not as a whole. Furthermore, the same value is calculated and presented for a location near but not at the error sensor.

5 ANC system simulations

Before the actual ANC system was built and tested, the different algorithms were first tested in simulations. The simulations were conducted in an environment programmed in Python. Goal of the simulations was to find algorithms and their parameters which could be suitable for the physical prototype system; thus, only local feedback ANC algorithms presented in Chapter 3 were simulated.

This chapter first explains the simulation system and the design choices made while programming it, after which the conducted simulations are introduced. Finally, results of these simulations are presented and discussed.

5.1 Simulation system description

5.1.1 Sampling frequency

The simulation system worked on sample-by sample basis on a sampling frequency of $f_s = 3000$ Hz. This sampling frequency was chosen for two reasons. First, using a high sample rate is a high computational burden to the ANC system. The used sample rate limits the usable bandwidth of the system by the Nyquist theorem, but as previously mentioned, local ANC systems are not expected to work at high frequencies. Using this sampling frequency sets the Nyquist frequency to 1500 Hz, which is higher than the upper limit where the system is expected to work in the first place. Second, it is convenient that the sample rate conversion from the prototype system's audio interface to the ANC algorithm is done with an integer ratio. As the chosen audio interface works with a sample rate of 48 kHz, the decimation from the audio interface to the ANC system and later interpolation from the ANC system back to the audio interface can both be done with conversion ratio of 16.

5.1.2 Secondary path impulse response

In contrast to a physical, real-world system, it is possible to simulate the exactly same impulse response for both the secondary path response S and its estimate $\hat{S}$; in addition, any kind of impulse response can be applied instead of just realistic ones. To test how the system behaves in both ideal and realistic settings, the simulations were conducted with three different kinds of secondary path impulse responses:

- Unit impulse response,
- Anechoic impulse response (room impulse response in an anechoic room), and
- Room impulse response of an ordinary office room.

The simulations didn't use real, measured impulse responses: the first is a simple unit impulse, and the latter two impulse responses were synthesized with the help of a Matlab program introduced in [43] instead. All three impulse responses are shown in Figure 15.

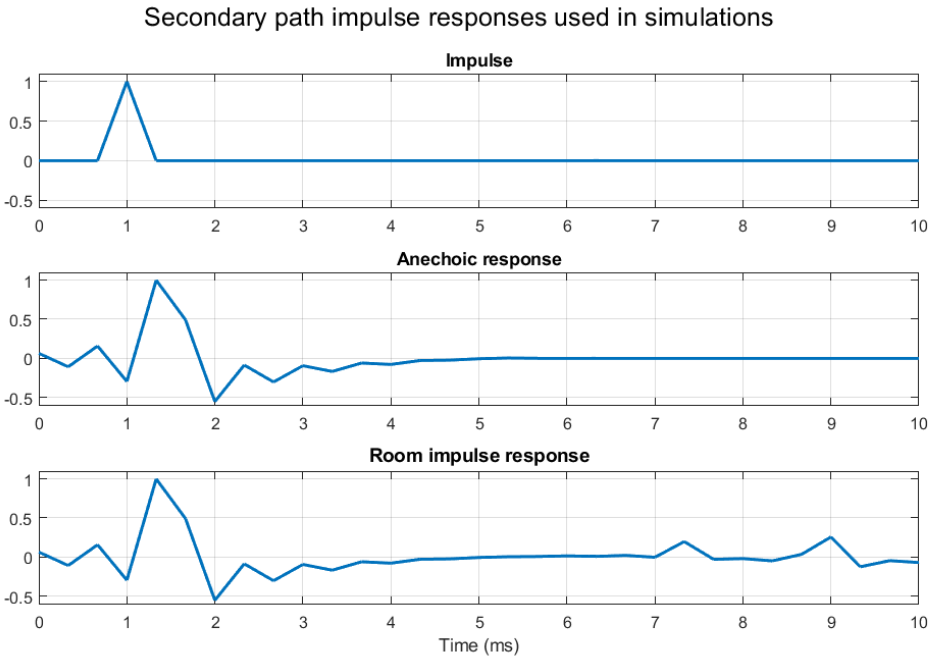

Figure 15: Secondary path impulse responses used in simulations.

5.1.3 Frequency weighting

As discussed earlier, active noise control is more effective at lower than it is at higher frequencies; however, the LMS algorithm does not discriminate between frequencies, and only aims to minimize the expected squared error signal $\mathbb{E}\left[e(n)^2\right]$ over the whole frequency range. As it is unlikely that the system would be able to control high frequencies in the first place, the system was decided to include an option to emphasize low frequencies over high frequencies by weighting the signals appropriately. This weighting was applied by introducing a few identical low-pass filters $LP(z)$ to the system, as shown in Figure 16. The Figure 16 shows the filters incorporated to the basic FxLMS IMC structure, but a similar structure was used to add them to the other algorithms as well.

The point of the different filters are as follows. One of these filters (1) was introduced in conjunction with the secondary path S so that the produced anti-noise would not contain high frequencies, and another filter (2) was introduced before the error signal was fed into the LMS algorithm so that the error signal seen by the LMS algorithm would not contain high frequencies, either. These two extra filters effectively transforms the secondary path seen by the LMS algorithm into $S_{eff}(z) = LP(z)S(z)LP(z)$. Therefore, for the secondary path estimate to accurately estimate this new secondary path, two of these low-pass filters were then cascaded into the secondary path estimate $\hat{S}$ leading to the LMS algorithm as well (3). The low-pass filters were implemented as 6th-order Butterworth infinite impulse response (IIR) filters with the cut-off points at 700 Hz.

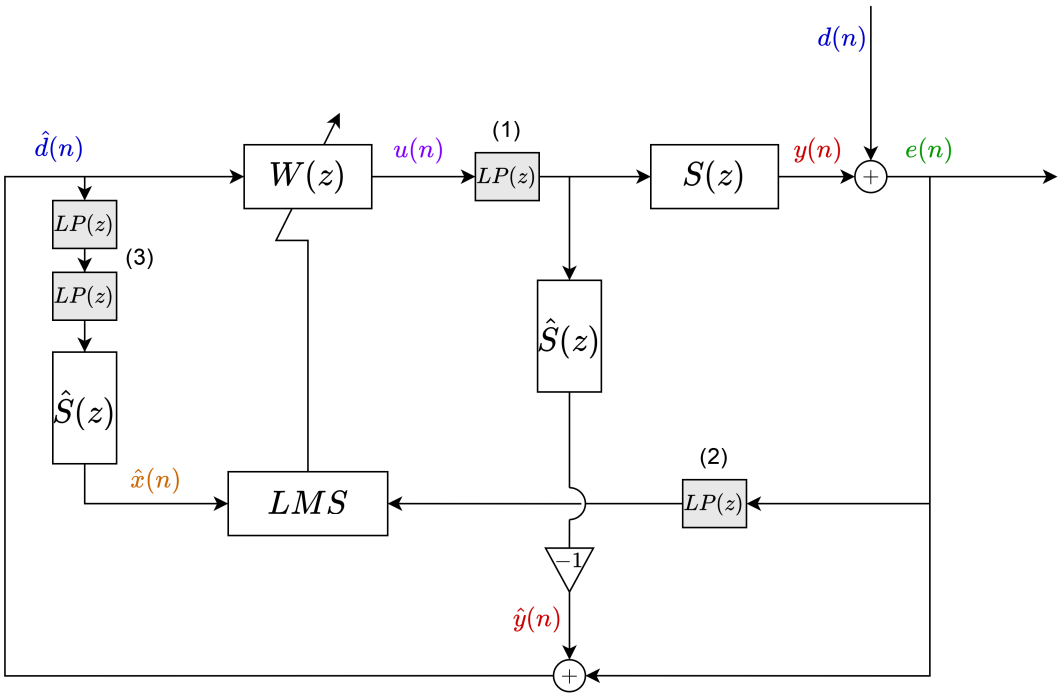

Figure 16: IMC structure with added low-pass filters $LP(z)$ for frequency weighting. (1): Filter out high frequencies from the anti-noise. (2): Filter out high frequencies from the error signal. (3): Align the phase responses of effective secondary path $S_{eff}(z) = LP(z)S(z)LP(z)$ and the secondary path estimate $\hat{S}$.

5.1.4 Algorithms

All the simulated algorithms contain one or more adaptive filters and corresponding LMS controllers. These controllers were chosen to be leaky normalized LMS controllers introduced in Section 3.4. These algorithms were also tested with the leaky factor $\gamma = 0$, reducing the controllers to the normalized LMS introduced in Section 3.2. All the tested algorithms apply the internal model control (IMC) FxLMS architecture introduced in Section 3.5.

Some preliminary testing was done to find a range of parameters with which the algorithms worked reasonably well on the different test signals. Based on these, a few values were chosen for each of them for the final simulations. Each combination of these parameters was then simulated on each test signal, to be explained in Section 5.2, and additional environmental parameters, to be explained in Section 5.1.5. For simplicity, the parameters L, μ and γ were kept the same for all the $2K + 1$ NLMS controllers in FLANN algorithm and the 2^K NLMS controllers in Wavelet algorithm. Furthermore, each algorithm was tested both with and without the frequency-weighting filters introduced in Section 5.1.3. Table 1 summarizes the different algorithms and shows the different algorithm parameter values to be simulated.

There are multiple different wavelet functions that can be used with the wavelet packet decomposition. In this thesis, the simplest one, *Haar*, was used. This wavelet

Table 1: Algorithms and their parameters chosen for simulations.

Algorithm	Introduced in	Parameters		Simulated values
LFxLMS	3.4, 3.5	Step size	μ	0.005, 0.01, 0.03
		Adaptive filter length	L	256, 512, 768, 1024
		Leaky factor	γ	0, 0.001
		Frequency weighting	LP	True, False
FLANN	3.6	Step size	μ	0.005, 0.01, 0.03
		Adaptive filter length	L	256, 512, 768, 1024
		Leaky factor	γ	0, 0.001
		Controller order	K	1, 2, 3
		Frequency weighting	LP	True, False
Wavelet	3.7	Step size	μ	0.005, 0.01, 0.03
		Adaptive filter length	L	256, 512, 768, 1024
		Leaky factor	γ	0, 0.001
		Controller order	K	1, 2, 3
		Frequency weighting	LP	True, False

function incorporates two-tap FIR filters for both the low-pass and high-pass filters [44], making the wavelet simple both conceptually and computationally. Figure 17 shows the FIR filter coefficients for Haar wavelet.

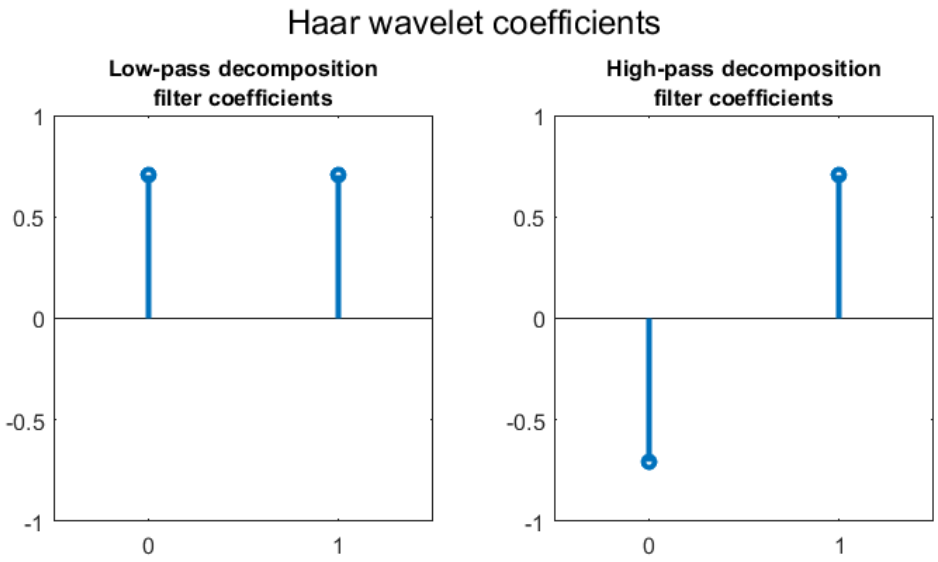

Figure 17: Haar wavelet filter coefficients.

5.1.5 Other controlled variables

In addition to the parameters governing the ANC operation, the simulation environment was built such that following environmental variables could also be controlled:

- Error microphone signal-to-noise ratio SNR, implemented with adding white Gaussian noise to the measured error signal,
- Secondary path impulse response S, ranging from a single unit impulse to a impulse response in an anechoic room to a real room impulse response (as introduced in 5.1.2),
- Latency of the secondary path Δ_S, adding zeroes to the beginning of the secondary path impulse response to achieve the desired latency in milliseconds,
- Temporal estimation error of the secondary path estimation S_{err}, padding the beginning of the estimated secondary path $\hat{S}$ with zeroes (but not the real secondary path S).

As stated earlier, each combination of these values was then simulated with each combination of the actual ANC algorithm parameters explained in the previous section. Table 2 shows the different simulated values for each of these parameters.

Table 2: Environmental variables and their values used in simulations.

	Variable	Simulated values
SNR	Error microphone signal-to-noise ratio	100 dB, 3 dB
S	Secondary path impulse response	impulse, anechoic, room
Δ_S	Secondary path latency	0 ms, 4 ms, 8 ms
S_{err}	Temporal error of secondary path estimation	0%, 1%

5.2 Test signals

The collection of test signals were chosen such that they would represent different signal types and system use scenarios. The chosen signals were:

1. Low-frequency fan noise,
2. Classical music,
3. Traffic noise,
4. Speech.

The system was also tested with other signals to get basic understanding of the behaviour and performance of the algorithms. These four signals were chosen for this report due to them including both signals that the system performed well and poorly on.

Table 3 summarizes and Figure 18 shows spectrograms of the test signals.

Table 3: Summary of the different test signals.

Signal	Description	Characteristics
Fan	Low-frequency ventilation noise	Strong tonal components at low frequencies, noisy on higher frequencies
Music	Symphony orchestral music	Slowly time-varying, relatively strong tonal components
Traffic	Traffic noise recorded by a busy urban road	Time-varying, most energy on low frequencies, noisy
Speech	Male person holding a speech	Time-varying, parts of silence in between, no long frequency components

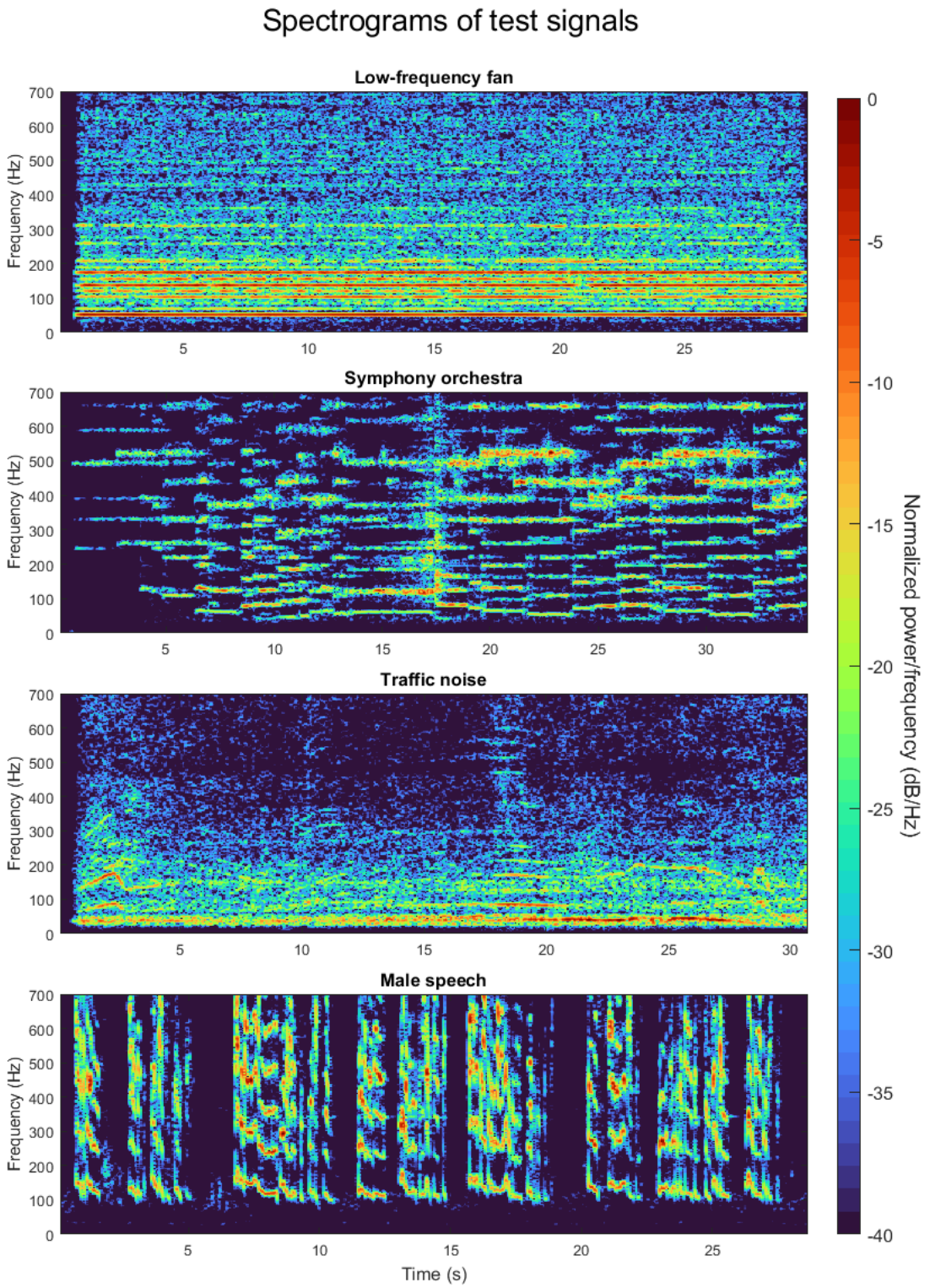

Figure 18: Spectrograms of the used test signals. Each spectrogram is normalized such that the highest value of the said spectrogram is at 0 dB.

5.3 Results

5.3.1 Attenuation with moderate secondary path latency

As the physical prototype system was bound to have some significant latency in its secondary path, the focus is here given to the simulations with 4 ms of secondary path latency, with the aim of presenting somewhat realistic results instead of ideal ones. Out of all simulations conducted, the best-performing set of ANC system parameters was found for each combination of test signal, ANC algorithm and secondary path response, with the limitation of secondary path latency being 4 ms. All the numerical results were calculated as the equivalent level difference between primary noise and error signals, given by equation 27. Refer to Section 5.1.4 on the different algorithms, Section 5.2 on the test signal description, and Section 5.1.2 on the secondary path responses.

The Table 4 shows the simulation results given separately for each test signal. Table 4a shows the performance on fan noise, Table 4b on symphony orchestra music, Table 4c on traffic noise, and Table 4d on male speech signal.

Table 4: Simulated attenuation of different test signals with different ANC algorithms and secondary path responses, given in decibels.

(a) Fan noise.

Algorithm	Impulse	Anechoic	Room
LFxLMS	8.57 dB	**8.51 dB**	8.01 dB
FLANN	8.12 dB	8.31 dB	7.07 dB
Wavelet	**8.60 dB**	8.50 dB	**8.11 dB**

(b) Orchestral music.

Algorithm	Impulse	Anechoic	Room
LFxLMS	**4.22 dB**	**3.94 dB**	**3.64 dB**
FLANN	2.02 dB	2.00 dB	1.72 dB
Wavelet	2.65 dB	2.37 dB	2.09 dB

(c) Traffic noise.

Algorithm	Impulse	Anechoic	Room
LFxLMS	**3.96 dB**	**3.23 dB**	**2.94 dB**
FLANN	2.87 dB	2.86 dB	2.38 dB
Wavelet	3.91 dB	3.10 dB	2.93 dB

(d) Speech.

Algorithm	Impulse	Anechoic	Room
LFxLMS	**0.89 dB**	0.55 dB	0.48 dB
FLANN	-10.68 dB	0.15 dB	-4.75 dB
Wavelet	0.80 dB	**0.56 dB**	**0.49 dB**

5.3.2 Effect of the secondary path latency

In addition to the parameters introduced in Table 1, additional simulations were conducted to find the effect of secondary path latency to the performance of the noise control. Figure 19 shows the simulated maximum attenuation on different secondary path latencies. The simulation used the basic FxLMS algorithm with a unit impulse as secondary path, and perfect secondary path estimation. Each signal was simulated with many different parameters for L and μ in addition to the secondary path latency, out of which the best performed combination was chosen for the said signal and latency to be shown in Figure 19.

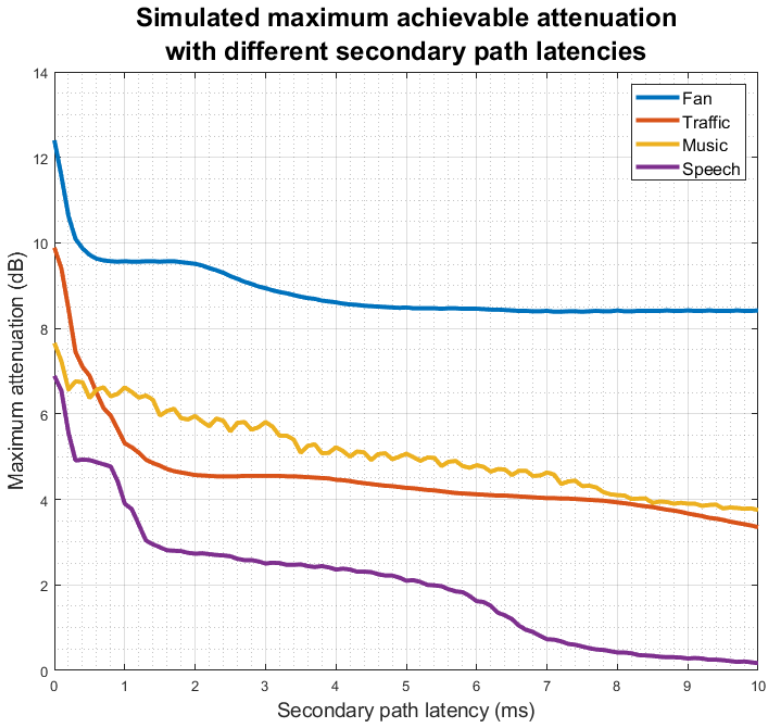

Figure 19: Maximum achievable attenuation of the test signals on different secondary path latencies based on simulations.

The Figure 19 shows that increasing latency on the secondary path negatively affects the performance of ANC on all signals, as expected from the theory covered in Sections 3.3 and 3.5. However, the effect is more severe on the quickly changing signals, such as speech, than on the steady fan signal.

It should be noted that the simulation is idealized in multiple ways. First, the secondary path response is idealized as a unit impulse, and its estimate is perfect. Second, the FxLMS parameters for each latency and signal were simulated with many combinations of adaptive filter length L and step size μ. Out of all these simulations, the attenuation was calculated with equation 27, and the best of all these values was chosen for the figure for each combination of test signal and secondary path latency. A real system would not be able to choose such best combination by trial and error, and would most probably be forced to settle for a worse combination.

5.4 Discussion and conclusion of simulation results

Generally, the unit impulse secondary path response achieved the best results, but such a system is very idealized. Thus, those results can be used as a guide on the theoretical upper limit of the performance, but they are not reproducible in real life. The anechoic and especially room impulse responses are better estimates on how the system would operate in a real setting, and should be interpreted as such. The following discussion focuses on the results from room impulse response simulations.

Out of all the test signals, all algorithms performed best on the fan noise and worst on the speech. This aligns well with the expected results, as feedback ANC systems tend to work better on predictable than on unpredictable signals. As the fan noise has strong, steady tonal components, the feedback controller was able to track those frequencies well. The traffic noise signal has its energy condensed on the lower frequencies, but is still rather noisy; furthermore, even the components on lower frequencies have some random behaviour. This results in a worse, but overall still quite good performance, compared to the fan noise. The orchestral music has strong tonal components, which can be tracked and predicted well, but it also contains random components which the system could not predict. Depending on the used algorithm, the resulting attenuation was generally of similar magnitude than with the traffic noise. Finally, the speech signal varies quickly in time, leading to more difficult tracking by the feedback controller, and thus worse results.

A key result from the simulations is that the secondary path latency has a much more severe effect to the performance with the rapidly changing signals than with the quasi-steady ones, as can be seen in Figure 19. This is due to the controller being able to predict the upcoming fan noise reliably even 10 ms into the future, as the signal is hardly changing in time. Conversely, the controller cannot predict the speech signal with the same delay, as the signal does appear to behave randomly when predicted that far into the future.

Out of the different algorithms, the basic LFxLMS performed best despite its simple architecture; the Wavelet algorithm did outperform LFxLMS on a few occasions, but the difference was small even in those situations. This is a somewhat curious result, as previous results have shown subband ANC significantly outperfoming the systems with only one band, and previous researches in [39] and [40] have reported the other two algorithms outperforming the basic FxLMS. There are a few possible explanations to this, though. First, the results from LFxLMS algorithm generally had one or a few combination of algorithm parameters with good performance with the rest of the combinations having much weaker results, while the performance of Wavelet algorithm was more stable across more combinations of parameters. This suggests that while LFxLMS can work really well when given the right parameters for the given primary signal and secondary path response, the performance drops rapidly if given suboptimal parameters. Second, the simulations used the same parameters for all 2^K NLMS controllers in the Wavelet algorithm. Optimizing these parameters separately could be used to achieve better results.

The FLANN algorithm was significantly underperforming in the simulations. It performed nearly as well as the other two algorithms on most of the signals, but even then was outperformed by the other two; moreover, it performed really poorly with the speech signal. The FLANN algorithm was designed to perform well with non-linear chaotic noise [39], however, the simulation system didn't introduce any nonlinearities to the signals. This means that the full potential of the FLANN algorithm was possibly not unleashed in these simulations. Furthermore, as with the Wavelet algorithm, better results could have been achieved were the different $2K + 1$ NLMS controllers optimized separately from each others.

The order of the Wavelet controller had little impact on the results, as the results on each of the three tested orders were within about 0.2 dB on each test signal and secondary path response type. This means that while the higher-order controller performed better on average, it is not clear if this difference makes it worth the increased computational cost. On the other hand, the FLANN controller had a better result with the first-order controller than with second or third order controller with all signals and secondary path responses, which further suggests the possibility of performance enhancement by optimizing the NLMS controllers' parameters separately, as less weight could then be given to the higher-order controllers. The introduction of the frequency weighting filters had varying effects on the different algorithms. Generally, LFxLMS performed better without them, while Wavelet and FLANN performed better with the filters. This effect of the filters was relatively small on the Wavelet algorithm and larger with the FLANN algorithm performance.

The simulations also tested the effect of the other environmental variables to the achievable attenuation. It was found that the simulated 1% temporal error on the secondary path estimation had virtually no effect on the results. This is well aligned with the rule of thumb that secondary path estimation phase errors up to 40° have little to no effect on the FxLMS performance. The error microphone signal-to-noise ratio had a small effect on the results depending on algorithm, signal, and secondary path response. This effect varied between 0.1 dB – 1.0 dB, and all algorithms were quite robust against the low SNR, though in some situations better results were achieved by some other combination of ANC parameters due to the lower SNR.

The simulations aligned well with the available theory. To summarize the results, the best algorithms performed very well on the steady fan noise, attenuating it by over 8 dB, and relatively well on the orchestral music and traffic noise, attenuating them by around 3.6 dB and 2.9 dB, respectively. However, the rapidly changing speech signal acquired just around 0.5 dB of attenuation at best. It was also confirmed that the latency imposed by the secondary path is a major bottleneck in the performance of an ANC system, and should be of big concern when designing one.

The simulations were idealized in many fronts compared to a real system, and thus it is expected that these results set an upper limit on the best possible performance on the real system. Based on the simulations, FxLMS and Wavelet algorithms were chosen to be implemented for the prototype system. The FLANN algorithm worked reasonably well on all signals except for the speech signal, but it was still the worst algorithm of the three in all four test signals. Even though the higher-order Wavelet algorithms generally outperformed the first-order controller, the effect of the controller order was so small, that the prototype system was decided to only implement the first-order Wavelet algorithm. Furthermore, as the frequency weighting had only little impact on the result, it was decided to be left out from the prototype system tests.

6 Prototype system construction and tests

Based on the simulation results, the best-performing algorithms and their parameters were tested with a prototype system, comprising of loudspeakers, microphones and a controller. The previous chapter presented the simulation results and justified which algorithms to be tested in this real system. This chapter first introduces the test environment and setup, and then explains how the measurements were made and their results. Finally, the results are discussed and reflected on the design choices and thesis goals.

6.1 Prototype system description

6.1.1 Physical setup

Figure 20 shows the schematic diagram of the measurement setup. The test setup includes two loudspeakers, one for the primary and one for the secondary noise. In addition, two microphones are included, one of them being the error microphone used to provide error signal for system control. LMS-based algorithms only try to cancel the sound at the error microphone location, but nothing is guaranteed at other locations. Thus, the other microphone acts as a control microphone, located at a fixed distance from the error microphone, to get a realistic estimate on how much the sound would be reduced at a location near but not at the error microphone. These devices were interfaced to the controlling laptop with a RME Fireface UCX audio interface.

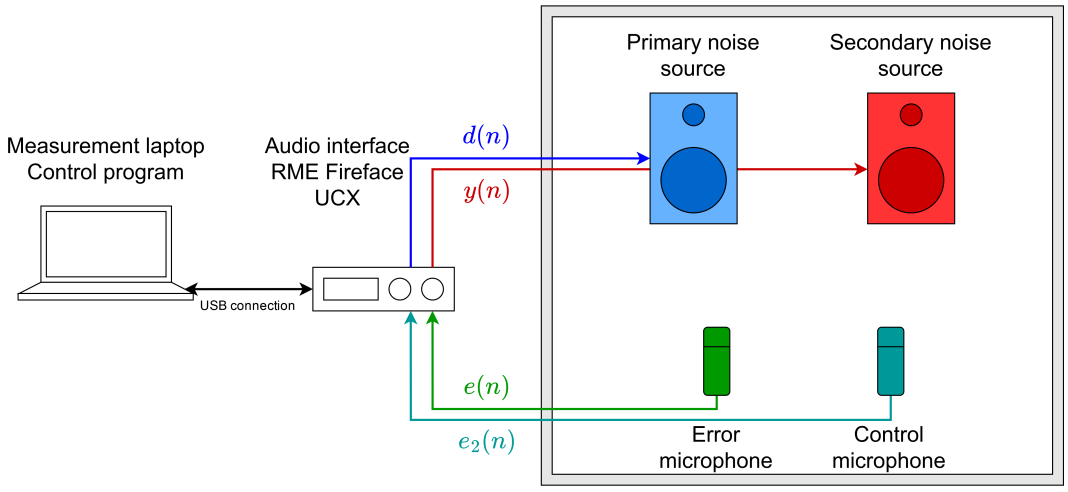

Figure 20: Schematic diagram showing the measurement setup.

6.1.2 Control program

The control software was programmed with C++ with the help of audio library Juce [45]. Before each test the secondary path impulse response would be calculated with an exponential sine sweep, after which the system could be run in two modes, either with or without ANC. In both settings, the system would play out a chosen test signal from the primary source loudspeaker and record the output of both of the microphones. When ANC was off, the secondary loudspeaker would stay silent; when it was on, the system would conduct the ANC with the given algorithm and play out the anti-noise signal from the secondary source loudspeaker. The program also included an interface to set the ANC system parameters adaptive filter length L, step size μ and leaky factor γ.

The audio interface worked at a sampling rate of 48 kHz, which is too expensive computationally for the ANC system to work in real time. Therefore, the input signal with the sample rate of 48 kHz was decimated with a factor of 16, resulting with the sample rate of 3000 Hz used by the ANC system, the same as in the simulations. The resulting anti-noise signal was interpolated with a factor of 16 to again result in a signal with sample rate of 48 kHz. Both the decimation and interpolation were done with the help of C++ library zita-resampler [46].

Figure 21 shows the logic of the control program.

6.1.3 Measurement locations

The measurements were made in three locations. To get an optimal reference result, the measurements were first made in the anechoic room Köykkä at Aalto University's acoustics lab. In addition, the system was tested in a small office room and in a light-weight phone booth, both located at Otakaari 5, Espoo.

Figure 22a shows the test setup in the anechoic room, Figure 22b in the office room, and Figure 22c in the phone booth. Figure 23 shows the secondary path impulse responses $\hat{S}$ measured from the test sites.

6.1.4 Limitations compared to the simulations

The two major differences between simulations and real-world tests had to do with secondary path estimation and the system latency. Whereas simulated system could perfectly estimate the secondary path, that is impossible to achieve in a real system. The secondary path impulse response was measured with an exponential sine sweep before each test, and the said impulse response was used as the secondary path estimation; thus, the estimation can be considered to be very accurate.

It has already been discussed multiple times on this thesis that the latency of the secondary path is the main limiting factor of a feedback ANC system. Whereas the latency imposed by the secondary path could be freely chosen in the simulations, the prototype system doesn't include the option to control it in any other way than by moving the microphones relative to the secondary source. Therefore, the system was not tested on different secondary path latencies. The audio interface used buffers of 48 samples, which equals to 1 ms of latency in both in- and outputs. Furthermore,

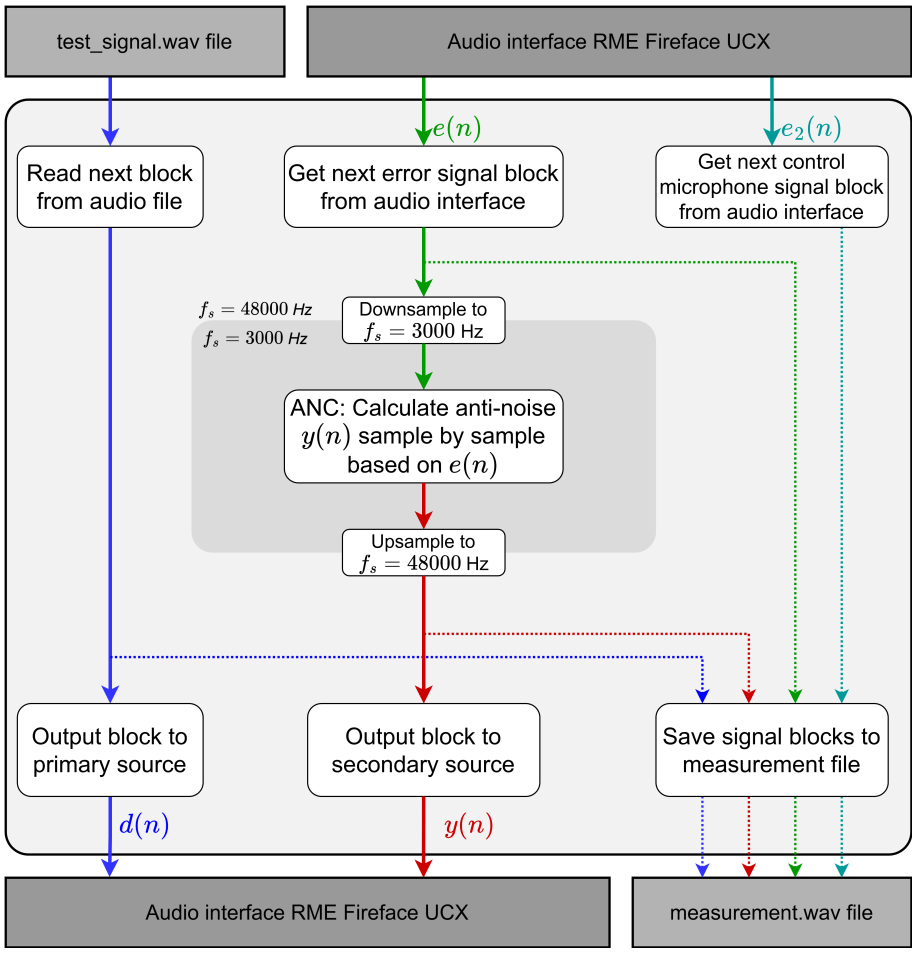

Figure 21: Flow diagram showing the operation logic of the control program.

the resampler used buffers which equals to roughly 2.7 ms in both decimation and interpolation. Thus, the total latency of the system is roughly 7.4 ms, not including digital-to-analog and analog-to-digital conversions or the acoustic travel time of the sound from the secondary source to the error microphone.

Section 5.3.2 and Figure 19 showed how the varying secondary path latency affected the system performance in the simulations, and those results can be used to estimate how the performance of the prototype system would improve were the latency lowered.

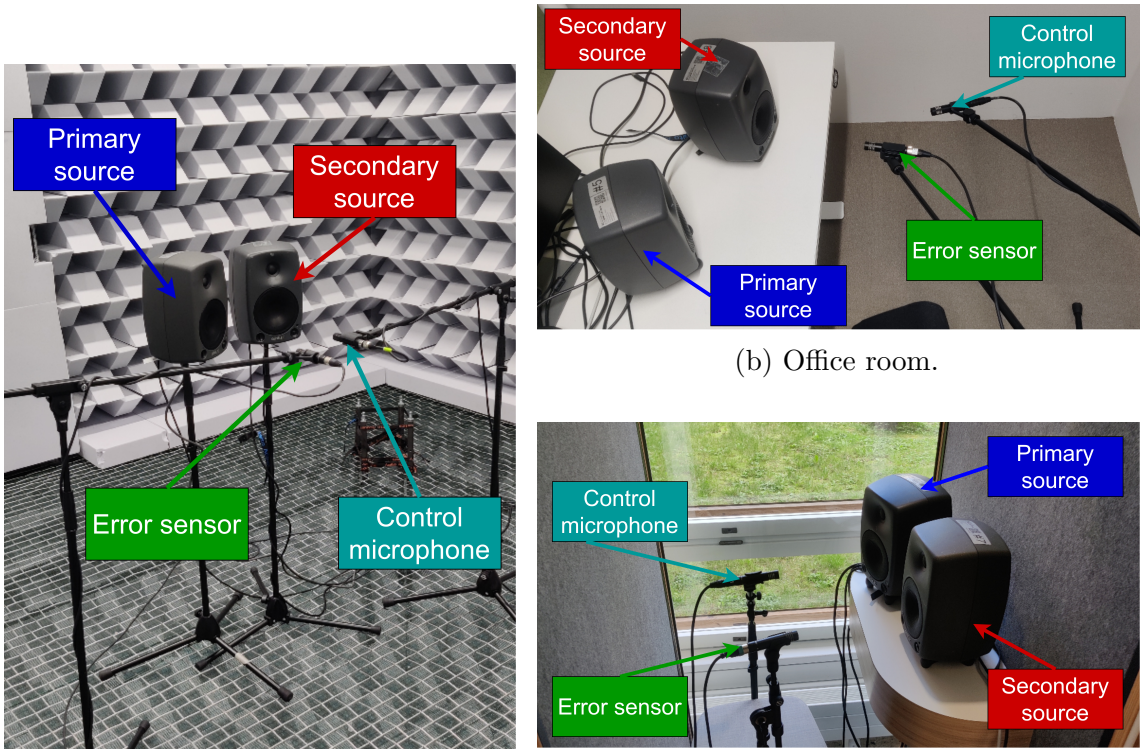

(a) Anechoic room.

(b) Office room.

(c) Phone booth.

Figure 22: Test setup in the different test locations.

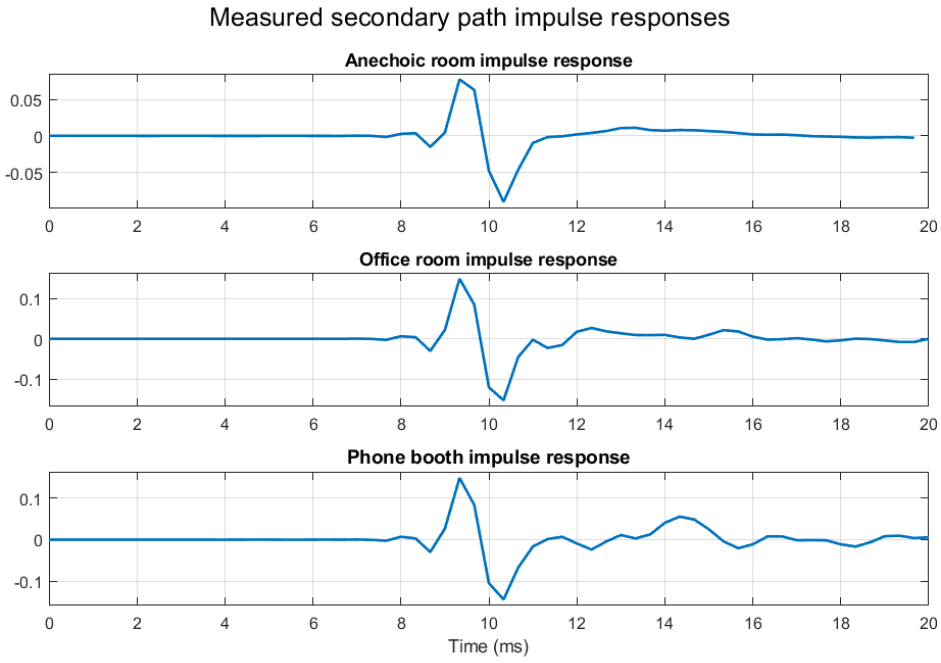

Figure 23: Secondary path impulse responses of measurement locations measured with an exponential sine sweep. Note the varying scale on the y-axes.

6.1.5 Measurement procedure

Each measurement set was done with the following procedure:

1. Measure the secondary path impulse response with an exponential sine sweep.
2. Choose a test signal and run the measurement without using the ANC (secondary source is silent), and save the output signal d and input signals e_{off} and $e_{2,off}$.
3. Choose the ANC algorithm and set ANC algorithm parameters L, μ and γ.
4. Run the measurement with ANC (secondary source emits the calculated anti-noise), and save the output signals d and y and input signals e_{on} and $e_{2,on}$.
5. Repeat steps 3 and 4 for each subsequent set of ANC parameters to be tested.
6. Repeat steps 2-5 for each subsequent test signal.

The raw error signal levels can change drastically between different rooms and furthermore are dependent on the test signal sound levels, and are thus not comparable as such. Instead, the interesting phenomenon under examination is how the sound level changes when switching ANC on, relative to the original sound level when ANC was not used. The underlying assumption of the procedure above is that the conditions of the room do not significantly change between conducting the test without and with ANC. With this assumption, the error signals of the two tests – without and with ANC – can together be used to determine how much the sound level changed in the room between not using and using the ANC system.

In the Figures 20 and 21 the primary noise generated by the test program was labeled as the primary noise $d(n)$ and the anti-noise as $y(n)$. This was done for convenience but it is not strictly correct, as d and y actually depict how the primary noise and anti-noise, respectively, behave *at the measurement location*, not what is produced in the first place. This means that the error signal $e_{off}(n)$ of the test without ANC is the correct interpretation of the real primary noise $d(n)$. This is taken into account in the subsequent sections by re-labeling the error signal of the test without ANC, $e_{off}(n)$ as the primary noise $d(n)$, and the error signal of the test with ANC, $e_{on}(n)$ as the error signal $e(n)$.

6.2 Results

The computational burden proved to be too much for the test program. This caused it to drop some audio blocks, resulting in audible clicks from the secondary loudspeaker. One consequence of this was that the program was not able to record the whole error signal, and had some blocks left out. This means that the primary and error noises cannot be compared directly, as they are no longer perfectly aligned in time. However, as the formula 27, with which the results are calculated with, averages the squared pressures *before* comparing the two signals to each other, this should

not affect the results much, but should still be keeped in mind when reviewing the results.

Similar to simulations, out of all measurements conducted, the best-performed set of ANC system parameters were found for each combination of test signal, ANC algorithm and measurement location. All the numerical results are calculated as the equivalent level difference between primary noise and error signals, given by equation 27. Refer to Section 5.1.4 on the different algorithm parameters, Section 5.2 on the test signal description, and Section 6.1.3 on the measurement locations.

The Table 5 shows the measurement results given separately for each test signal. Table 5a shows the performance on fan noise, Table 5b on symphony orchestral music, Table 5c on traffic noise, and Table 5d on male speech signal. Figure 24 shows the power spectral density differences between primary noise and error signals in the anechoic room measurement with the Wavelet algorithm.

Table 5: Measured attenuation of different test signals at the error microphone with different ANC algorithms in different test sites, given in decibels.

(a) Fan noise.

Algorithm	Anechoic room	Office room	Phone booth
LFxLMS	6.41 dB	4.32 dB	6.48 dB
Wavelet	**6.60 dB**	**4.85 dB**	**6.78 dB**

(b) Orchestral music.

Algorithm	Anechoic room	Office room	Phone booth
LFxLMS	1.41 dB	0.76 dB	0.77 dB
Wavelet	**1.97 dB**	**2.30 dB**	**2.99 dB**

(c) Traffic noise.

Algorithm	Anechoic room	Office room	Phone booth
LFxLMS	0.70 dB	1.17 dB	**1.22 dB**
Wavelet	**0.89 dB**	**1.45 dB**	1.20 dB

(d) Speech.

Algorithm	Anechoic room	Office room	Phone booth
LFxLMS	-0.13 dB	0.20 dB	-0.89 dB
Wavelet	**0.09 dB**	**0.64 dB**	**-0.28 dB**

The sound pressure was also measured with a control microphone, which was located at 20 cm from the error microphone, as seen in Figures 22a, 22b and 22c. Table 6 shows the results of the attenuation at this control microphone. Note that as

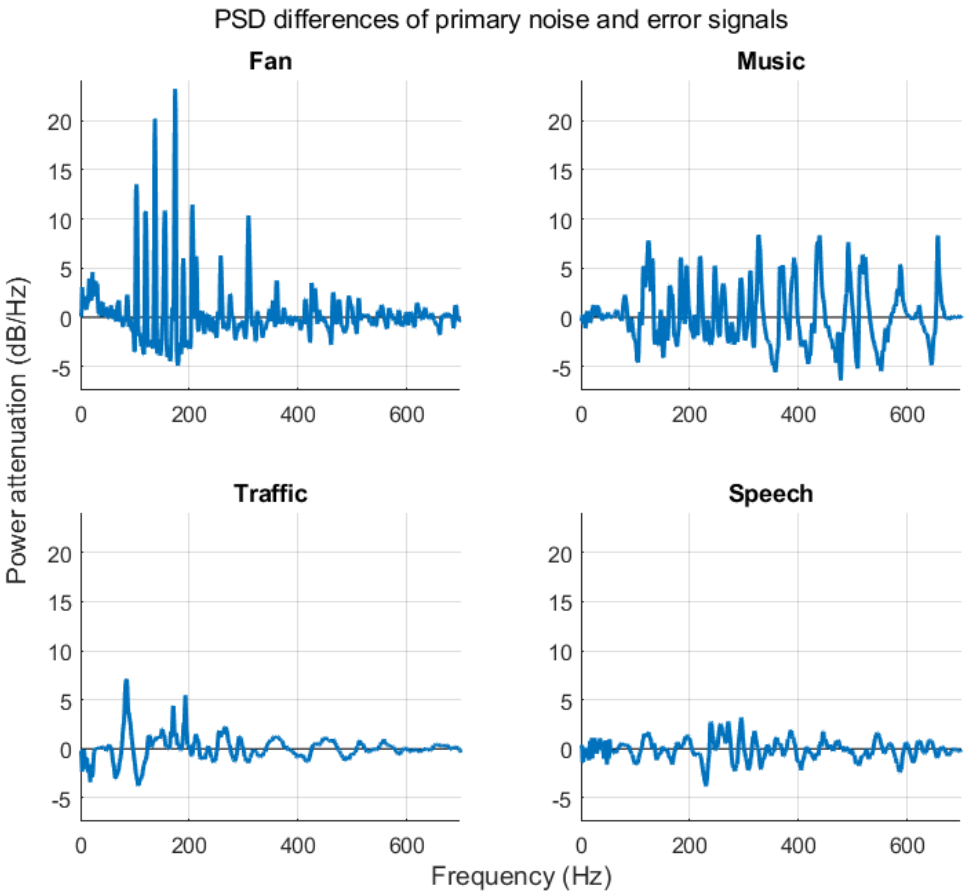

Figure 24: Welch power spectral density estimate differences between primary noise and error signals of different test signals. Signals are from the measurements conducted in the anechoic room with the Wavelet algorithm. High peaks mean large attenuation, while values less than zero mean that the primary noise was amplified by the secondary noise.

all the different test sites had a different configuration and the positioning between primary source, secondary source, error microphone and the control microphone was not exactly the same, the results are not comparable between test sites. However, they still give some insight on how the sound field behaves near the error microphone in each measurement location.

Table 6: Measured attenuation of different test signals at the control microphone with different ANC algorithms in different test sites, given in decibels.

(a) Fan noise.

Algorithm	Anechoic room	Office room	Phone booth
LFxLMS	1.20 dB	4.04 dB	2.61 dB
Wavelet	1.20 dB	**4.44 dB**	**2.65 dB**

(b) Orchestral music.

Algorithm	Anechoic room	Office room	Phone booth
LFxLMS	-0.39 dB	0.05 dB	**0.21 dB**
Wavelet	**0.55 dB**	**1.11 dB**	0.18 dB

(c) Traffic noise.

Algorithm	Anechoic room	Office room	Phone booth
LFxLMS	0.03 dB	1.39 dB	0.92 dB
Wavelet	**0.07 dB**	**1.62 dB**	**0.96 dB**

(d) Speech.

Algorithm	Anechoic room	Office room	Phone booth
LFxLMS	-0.36 dB	0.25 dB	-0.43 dB
Wavelet	**-0.30 dB**	**0.51 dB**	**-0.16 dB**

6.3 Discussion

The attenuation on different signals behaved as expected based on the simulations. The attenuation is the greatest with the fan noise, with which the total attenuation could be over 6 dB, depending on the test site. This kind of attenuation is relatively good and certainly audible. Furthermore, the orchestral music achieved almost 3 dB of attenuation, which also is audible. Conversely, the traffic noise was attenuated by only around 1 dB, and the speech signal had virtually no change to the original. One major cause for worse performance is the secondary path latency, which was around 9 ms in all test sites. It was already discussed with the simulation results that this kind of secondary path latency is a limiting factor, and thus, these results could be expected.

The primary noise sound level difference between error and secondary microphones were relatively large. On average, in the anechoic room, the primary noise level was 7 dB higher at the error microphone than at the control microphone; in the office room, the primary noise level was about 3 dB higher at the error microphone than at

the control microphone; and in the phone booth, the primary noise level was about 4 dB higher at the control microphone than at the error microphone. This is probably partly due to the directivity of the loudspeakers and microphones: more sound power radiated to the microphone directly in front of the loudspeaker than to the other one being slightly to the side. This partly explains the somewhat inconsistent-looking results shown in Table 6. As such, the results shown in Table 6 give some insight on how the sound field can behave near the error microphone, but the results are not comparable between each other.

Out of the two tested algorithms, the Wavelet performed better on almost all signals and test sites and lost only with a really small margin when LFxLMS performed better. Thus, Wavelet can be deemed better out of the two algorithms for this application.

For future work, the first thing to be considered is to lower the secondary path latency. As can be seen from Figure 19, the secondary path latency in the prototype system was about 9 ms, acoustic propagation time included. Most of the latency was caused by the sample rate conversion, and thus, a quicker method could be used. However, the computational burden of the algorithms was already too high to the test program. This issue could be improved by increasing the buffer size, which would unfortunately lead to an even bigger latency. On the other hand, the program was not optimized, and could potentially handle the active noise control if special care was put into it. Another limiting factor of the prototype system was the static ANC algorithm parameter values, whereas simulations could be run on a huge number of different combinations and choose the best out of those. In theory, some machine learning or artificial intelligent based approach could be used to control and optimize these parameters while the system is running.

One final important aspect to note is that all the tested algorithms were LMS-based and also previously researched. The fundamental problem of ANC is to produce anti-noise which very accurately has the same amplitude and inverted phase than the primary noise, at the measurement location. Feedback ANC systems have the additional limitation of only working with the samples from the past, and not having any other information of the upcoming samples than the statistics of the error signal. LMS-based alorithms offer a convenient way of predicting the upcoming noise, but as shown in the results, it has major limitations with broadband signals. If, somehow, the upcoming samples could be more accurately predicted into the future, then the problem of feedback ANC would essentially turn into a feed-forward one, simplifying the system quite a bit. However, such a method has not yet been developed.

To summarize the results, the system worked as expected. The noise attenuation was good, over 6 dB on the fan noise signal with strong tonal components, but much lower on the other signals with more time-varying contents. If only the multi-tonal fan noise was considered, the system could be argued to provide adequate attenuation, thus meeting the goals set for the system. However, when considering broadband noise, the results are reasonably good depending on the signal but nowhere near the comfort, easiness of use and noise attenuation level that active noise cancelling headphones provide. Thus, while the results did not outright deny the possibility of using a similar feedback ANC solution in the future, they did not give enough evidence

supporting the feasibility of using such a system, either. All things considered, this kind of system can not compete with the active noise cancelling headphones – silence in a bottle was not yet realized. Further study is thus required to truly move the buds out of ears.

7 Conclusion

The aim of this thesis was to evaluate the feasibility of using a mobile, easy-to-use active noise control (ANC) system in real 3D-spaces. The core idea behind the system was to provide the easiness of active noise canceling headphones without the user having to wear anything in their ears, while still providing adequate noise reduction. To achieve this goal, different ANC algorithms were simulated, after which two of those algorithms were tested with a physical prototype system.

ANC systems can be divided into feed-forward or feedback systems based on if they have a reference signal available or not, and into local, global or spatial systems based on the effective control area of the system. Even though feedback systems have major drawbacks compared to feed-forward ones, they remain as the only reasonable approach, as feed-forward systems require one or multiple coherent reference signals, which cannot be expected to be available in varying 3D-spaces. The effective area of this feedback controller was then decided to be local control, meaning that one discrete point in the room is being attenuated instead of the whole enclosure or a subspace of it. This was decided due to the other two approaches, global and spatial control, either requiring a large number of microphones and loudspeakers, or forcing the user to recalibrate the system for each new space they take it to. These requirements would lead the system too far away from the comfort of headphones.

Multiple least mean squares (LMS) based ANC algorithms were introduced. Out of these, three ANC algorithms were simulated using a simulation environment programmed in Python: leaky filtered-x least mean squares algorithm (LFxLMS), functional link artificial neural network -based LFxLMS (FLANN), and wavelet packet transform based LFxLMS (Wavelet). Out of these three, LFxLMS and Wavelet were then tested with a prototype system. The prototype system consisted of one secondary source and one error microphone in addition to a primary source playing out the primary noise for the measurement and an additional control microphone to measure how the sound field behaves near the error microphone, and they were controlled with a test software programmed with Juce. The measurements were conducted on three different test sites: in an anechoic room, in an office room, and in a light-weight phone booth. The system minimized the expected squared sound pressure at error microphone location, meaning that if such a system would be commercialized as such, the user would have to wear a microphone near their ears, limiting the practical use of the system. A few different virtual sensing techniques were briefly introduced, but they were not implemented to the prototype system in this thesis work.

The results showed that the system worked well on steady multi-tonal fan noise, achieving a total attenuation of about $L_{eq,Z} = 6$ dB. However, the system performed poorly on signals varying quickly in time, such as with speech signal. Secondary path latency was identified to be the main limiting factor of the system with the help of simulations. As the prototype system did not perform well on broadband noise, all the goals set for the system were not satisfied, and thus, the results did not support the feasibility of using a mobile, easy-to-use ANC system to reduce broadband noise at a single point in a 3D-space. In particular, the prediction capabilities of the

feedback controller was shown to be of a major consideration. However, the results cannot be interpreted to outright deny the possibility of developing such a system, either, as only a few relatively simple ANC algorithms were tested, all of them being based on the LMS algorithm. In addition, the prototype system was identified to include a major limitation in the form of a long secondary path latency.

Multiple possible improvements to the system were discussed. First, the secondary path latency should be minimized at all reasonable cost. Second, a hybrid approach could be used to obtain a reference signal from a dominant direction. Third, machine learning or artificial intelligence could be applied to the system by either having them tune the available parameters while the system is running, or to predict the incoming noise more accurately and further into the future than the linear FIR filters can. Finally, the scope of this thesis was limited to single-channel ANC, but incorporating multiple error sensors and secondary loudspeakers could improve the performance of the system. More research is thus needed to further understand the phenomena behind feedback ANC and to create a more optimal system.

References

[1] L. Goines and L. Hagler, "Noise pollution: a modern plague," *South Med J*, vol. 100, no. 3, pp. 287–294, Mar. 2007. DOI: 10.1097/SMJ.0b013e3180318be5.

[2] M. Basner, W. Babisch, A. Davis, M. Brink, C. Clark, S. Janssen, and S. Stansfeld, "Auditory and non-auditory effects of noise on health," *The Lancet*, vol. 383, no. 9925, pp. 1325–1332, Apr. 2014. DOI: 10.1016/S0140-6736(13)61613-X.

[3] B. Berglund, T. Lindvall, and D. Schwela, "New WHO guidelines for community noise," *Noise & Vibration Worldwide*, vol. 31, no. 4, pp. 24–29, Apr. 2000. DOI: 10.1260/0957456001497535.

[4] H. Jariwala, H. Syed, M. Pandya, and Y. Gajera. "Noise pollution & human health: a review." (Mar. 2017), [Online]. Available: https://www.researchgate.net/publication/319329633_Noise_Pollution_Human_Health_A_Review (visited on 09/23/2023).

[5] S. Kuo and D. Morgan, "Active noise control: A tutorial review," *Proceedings of the IEEE*, vol. 87, no. 6, pp. 943–973, Jun. 1999. DOI: 10.1109/5.763310.

[6] S. Elliott, "Down with noise [active noise control]," *IEEE spectrum*, vol. 36, no. 6, pp. 54–61, Jun. 1999. DOI: 10.1109/6.769270.

[7] P. Samarasinghe, W. Zhang, and T. Abhayapala, "Recent advances in active noise control inside automobile cabins: toward quieter cars," *IEEE Signal Processing Magazine*, vol. 33, no. 6, pp. 61–73, Nov. 2016. DOI: 10.1109/MSP.2016.2601942.

[8] M. Larsson, "Active noise control in ventilation systems: practical implementation aspects," Licentiate Thesis, Blekinge Institute of Technology, Karlskrona, Sweden, 2008. [Online]. Available: https://urn.kb.se/resolve?urn=urn%3Anbn%3Ase%3Abth-00423 (visited on 09/23/2023).

[9] C. Mak, W. To, T. Tai, and Y. Yun, "Sustainable noise control system design for building ventilation systems," *Indoor and Built Environment*, vol. 24, no. 1, pp. 128–137, Feb. 2015. DOI: 10.1177/1420326X13512144.

[10] B. Lam and W.-S. Gan, "Active acoustic windows: towards a quieter home," *IEEE Potentials*, vol. 35, no. 1, pp. 11–18, Jan. 2016. DOI: 10.1109/MPOT.2014.2310776.

[11] B. Lam, W.-S. Gan, D. Shi, M. Nishimura, and S. S. Elliott, "Ten questions concerning active noise control in the built environment," *Building and Environment*, vol. 200, article no. 107928, Aug. 2021. DOI: 10.1016/j.buildenv.2021.107928.

[12] L. Ang, Y. Koh, and H. Lee, "The performance of active noise-canceling headphones in different noise environments," *Applied Acoustics*, vol. 122, pp. 16–22, Jul. 2017. DOI: 10.1016/j.apacoust.2017.02.005.

[13] S. Liebich, J. Fabry, P. Jax, and P. Vary, "Signal processing challenges for active noise cancellation headphones," in *Speech Communication; 13th ITG-Symposium*, Oldenburg, Germany, Oct. 2018, pp. 1–5, ISBN: 978-3-8007-4767-2. [Online]. Available: https://ieeexplore.ieee.org/abstract/document/8577985 (visited on 09/23/2023).

[14] X. Shen, "Advanced active noise control headphone: algorithm and implementation," Ph.D. dissertation, Nanyang Technological University, Singapore, 2023. DOI: 10.32657/10356/166615. [Online]. Available: https://hdl.handle.net/10356/166615 (visited on 09/23/2023).

[15] J. Zhang, T. Abhayapala, W. Zhang, P. Samarasinghe, and S. Jiang, "Active noise control over space: a wave domain approach," *IEEE/ACM Transactions on audio, speech, and language processing*, vol. 26, no. 4, pp. 774–786, Jan. 2018. DOI: 10.1109/TASLP.2018.2795756.

[16] S. Ha, J. Kim, H. Kim, and S. Wang, "Horizontal active noise control-based wave field reproduction using a single circular array in 3D space," *Applied Sciences*, vol. 12, no. 20, article no. 10245, 2022. DOI: 10.3390/app122010245.

[17] P. Lueg, "Process of silencing sound oscillators," U.S. Patent 2 043 416, Jun. 9, 1936.

[18] D. Shi, B. Lam, W.-S. Gan, and J. Cheer, "Active noise control in the new century: the role and prospect of signal processing," *arXiv preprint*, Jul. 2023. DOI: 10.48550/arXiv.2306.01425.

[19] H. Olson and E. May, "Electronic sound absorber," *The Journal of the Acoustical Society of America*, vol. 25, no. 6, pp. 1130–1136, Nov. 1953. DOI: 10.1121/1.1907249.

[20] B. Widrow, J. Glover, J. McCool, J. Kaunitz, C. Williams, R. Hearn, J. Zeidler, J. E. Dong, and R. Goodlin, "Adaptive noise cancelling: principles and applications," *Proceedings of the IEEE*, vol. 63, no. 12, pp. 1692–1716, Dec. 1975. DOI: 10.1109/PROC.1975.10036.

[21] D. Morgan, "History, applications, and subsequent development of the FXLMS algorithm [DSP history]," *IEEE Signal Processing Magazine*, vol. 30, no. 3, pp. 172–176, Apr. 2013. DOI: 10.1109/MSP.2013.2242394.

[22] S. Elliott, *Signal Processing for Active Control*, 1st edition. London: Academic Press, 2001, ISBN: 0-12-237085-6.

[23] P. Nelson and S. Elliott, *Active Control of Sound*, 1st edition. London: Academic Press, 1993, ISBN: 0-12-515426-7.

[24] Centers for Disease Control and Prevention. "What noises cause hearing loss?" (2022), [Online]. Available: https://www.cdc.gov/nceh/hearing_loss/what_noises_cause_hearing_loss.html (visited on 08/04/2023).

[25] T. Kletschkowski, *Adaptive Feed-forward Control of Low Frequency Interior Noise*, 1st edition. London: Springer Science + Business Media, 2012, ISBN: 978-94-007-2537-9.

[26] S. Kuo and D. Morgan, *Active Noise Control Systems: Algorithms and DSP Implementations*, 1st edition. New York: John Wiley & Sons, 1996, ISBN: 0-471-13424-4.

[27] N. Zafeiropoulos, "Active noise control in a luxury vehicle," Ph.D. dissertation, University of Salford, Salford, United Kingdom, 2015. [Online]. Available: https://salford-repository.worktribe.com/output/1407558/active-noise-control-in-a-luxury-vehicle (visited on 09/23/2023).

[28] V. Patel, S. Bhattacharjee, J. Cheer, and N. George, "Hybrid feedback active noise control headset based on binaural signal utilization," *Applied Acoustics*, vol. 200, article no. 109062, Nov. 2022. DOI: 10.1016/j.apacoust.2022.109062.

[29] S. Elliott and T. T.J. Sutton, "Performance of feedforward and feedback systems for active control," *IEEE Transactions on Speech and Audio Processing*, vol. 4, no. 3, pp. 214–223, May 1996. DOI: 10.1109/89.496217.

[30] I. Jeong and Y. Park, "Suboptimal controller design of global active noise control system for various acoustic environments," *Scientific Reports*, vol. 13, article no. 5453, Apr. 2023. DOI: 10.1038/s41598-023-32261-9.

[31] G. Mangiante, "Active sound absorption," *The Journal of the Acoustical Society of America*, vol. 61, no. 6, pp. 1516–1523, Jun. 1977. DOI: 10.1121/1.381453.

[32] A. Montazeri, J. Poshtan, and M. Kahaei, "Modal analysis for global control of broadband noise in a rectangular enclosure," *Journal of Low Frequency Noise, Vibration and Active Control*, vol. 26, no. 2, pp. 91–104, Jun. 2007. DOI: 10.1260/026309207781894905.

[33] M. Schroeder and K. Kuttruff, "On frequency response curves in rooms. Comparison of experimental, theoretical, and monte carlo results for the average frequency spacing between maxima," *The Journal of the Acoustical Society of America*, vol. 34, no. 1, pp. 76–80, Jan. 1962. DOI: 10.1121/1.1909022.

[34] C. Kestell, B. Cazzolato, and C. Hansen, "Active noise control in a free field with virtual sensors," *The Journal of the Acoustical Society of America*, vol. 109, no. 1, pp. 232–243, Jan. 2001. DOI: 10.1121/1.1326950.

[35] J. Zhang, "Active noise control over spatial regions," Ph.D. dissertation, The Australian National University, Canberra, Australia, 2019. DOI: 10.25911/5d5148bcd6a10. [Online]. Available: http://hdl.handle.net/1885/161070 (visited on 09/25/2023).

[36] S. Haykin, *Adaptive Filter Theory*, 3rd edition. New Jersey: Prentice Hall, 1996, ISBN: 0-13-322760-X.

[37] H. Hassanpour and P. Davari, "An efficient online secondary path estimation for feedback active noise control systems," *Digital Signal Processing*, vol. 19, no. 2, pp. 241–249, Mar. 2009. DOI: 10.1016/j.dsp.2008.06.007.

[38] L. Lu, K.-L. Yin, R. de Lamare, Z. Zheng, Y. Yu, X. Yang, and B. Chen, "A survey on active noise control in the past decade–part II: nonlinear systems," *Signal Processing*, vol. 181, article no. 107929, Apr. 2021. DOI: 10.1016/j.sigpro.2020.107929.

[39] S. Behera, D. Das, and N. Rout, "Nonlinear feedback active noise control for broadband chaotic noise," *Applied Soft Computing*, vol. 15, pp. 80–87, Feb. 2014. DOI: 10.1016/j.asoc.2013.10.025.

[40] L. Luo, J. Sun, and B. Huang, "A novel feedback active noise control for broadband chaotic noise and random noise," *Applied Acoustics*, vol. 116, pp. 229–237, Jan. 2017. DOI: 10.1016/j.apacoust.2016.09.029.

[41] J. Jiang and Y. Li, "Review of active noise control techniques with emphasis on sound quality enhancement," *Applied Acoustics*, vol. 136, pp. 139–148, Jul. 2018. DOI: 10.1016/j.apacoust.2018.02.021.

[42] Y. Wang, L. Gu, F. Liu, and M. Dong, "An adaptive algorithm for nonstationary active sound-profiling," *Applied Acoustics*, vol. 137, pp. 51–61, Aug. 2018. DOI: 10.1016/j.apacoust.2018.03.002.

[43] E. Habets. "Room impulse response generator." Technical report. (Jan. 2006), [Online]. Available: https://www.researchgate.net/publication/259991276_Room_Impulse_Response_Generator (visited on 09/23/2023).

[44] F. Wasilewski. "Wavelet browser: Haar." (2022), [Online]. Available: https://wavelets.pybytes.com/wavelet/haar/ (visited on 09/24/2023).

[45] R. M. S. Limited. "Juce." (2023), [Online]. Available: https://juce.com/ (visited on 08/31/2023).

[46] F. Adriaensen. "Zita-resampler. GitHub repository." (2021), [Online]. Available: https://github.com/digital-stage/zita-resampler (visited on 08/31/2023).